Remobilizing surfactant retarded fluid particle interfaces. I. Stress-free conditions at the interfaces of micellar solutions of surfactants with fast sorption kinetics

Kathleen J. Stebe, Shi-Yow Lin, and Charles Maldarelli[a)]
The Levich Institute, Department of Chemical Engineering, City College of New York, New York, New York 10031

(Received 25 October 1989; accepted 27 August 1990)

Surfactant molecules adsorb onto the interfaces of moving fluid particles and are convected to regions in which the surface flow converges. Accumulation of surfactant in these regions creates interfacial tension gradients that retard the surface flow. In this study it is argued theoretically and demonstrated experimentally that fluid movement on the surface of a drop or bubble can remain unhindered in the presence of a single adsorbed surfactant if, relative to the convective rate of transport of adsorbed surfactant along the surface, desorption is fast, and the bulk concentration is high enough so that diffusion away from the particle is fast. For this circumstance, a uniform surface concentration of surfactant is maintained, and no gradients in surface tension arise to retard the surface velocity. The fluid particle flow behaves as it would in the absence of surfactant save that it has a reduced, uniform surface tension. The remobilization of surfactant-laden interfaces of fluid particles is demonstrated experimentally in a three-phase periodic slug flow in a capillary tube in which a train of alternating air and aqueous slugs ride on an annular wetting film of fluorocarbon oil. Surfactant, dissolved in the aqueous slug phase, adsorbs onto and retards the aqueous–oil interface. The hydrodynamics of this flow is such that small changes in the mobility of this interface create large shear rates in the oil layer. This significantly increases the pressure drop required to drive the slug train at constant velocity. Three surface adsorbers are used to demonstrate surface remobilization: The polyethoxy, nonionic surfactants Triton X-100 and Brij-35, which have fast desorption kinetics and do not retard the surface flow at high concentrations and, as a counter example, the desorption hindered protein bovine serum albumin, which is shown to be unable to remobilize an interface even at high concentration.

I. INTRODUCTION

Surfactant molecules which adsorb onto the interfaces of a translating fluid particle are convected toward stagnation regions where the surface flow converges. Accumulation of surfactant in the vicinity of these regions creates a surface pressure or Marangoni stress which is directed opposite to the direction of convection, and thus retards the surface velocity. This loss in interfacial mobility significantly affects the physicochemical hydrodynamics of the fluid particle flow. Among the many examples include the decrease in the rate of interphase mass transfer during dropwise extraction,[1] the reduction in the rate of thinning of the fluid between mutually approaching particles in an emulsion or foam,[2] the decrease in thermocapillary migration in a microgravity environment,[3] and the changes in foam mobility in capillary pore flows.[4,5]

This paper is the first of a two-part study concerned with understanding how surfactant retarded fluid particle interfaces can be remobilized. The aim of this part is to identify, by examining the mechanisms of surfactant transport, conditions where adsorption is not accompanied by a reduction in the surface velocity, and to verify these conditions with particular surfactants in a carefully controlled experimental fluid particle flow. The aim of the second part[6] is to examine the circumstance in which a surfactant impurity has retarded an interface, and to demonstrate how surfactants that are unretarding can, by competitive adsorption, displace the impurity from the surface and thereby remobilize the interface.

While more precise scaling arguments will be presented in what follows, it is at least qualitatively clear that desorptive and bulk diffusive resistances to exchange of surfactant between the bulk and the surface are what allows surfactant, concentrated by convection, to collect at converging stagnation points on the fluid particle surface. In the absence of these resistances, the surface concentration would be uniform, and Marangoni stresses would not retard the surface velocity. The central argument of this study is that the desorptive and bulk diffusive resistances can be eliminated under the following two conditions: First, the molecular desorption rate has to be fast in comparison to the prevailing convective rate at which surfactant is swept to the stagnation zone on the particle interface. Second, the bulk concentration must be high enough in order to eliminate a diffusion boundary layer resistance. The reason why sufficiently high concentrations of bulk surfactant can eliminate this resistance is explained in the following paragraph.

a) Author to whom correspondence should be addressed.

 0899-8213/91/010003-18$02.00

Surface convection in the vicinity of a converging stagnation region brings surfactant to that vicinity, and locally elevates the surface and bulk sublayer concentrations. The rate of this convective mass transfer (per unit length of surface perimeter cross sectional to the surface flow) scales with the magnitude of the product of the characteristic surface velocity and the surface concentration. The characteristic surface concentration can be taken to be Γ_0', the value which, with no flow, is in equilibrium with the bulk concentration C_∞'. (In this study, dimensional quantities are differentiated from nondimensional ones by a prime.) Bulk diffusion away from the particle surface can remove this excess surfactant, and the interfacial tension imbalance it creates. The rate of bulk diffusion (per unit area of surface) scales with the product of the diffusion coefficient and the bulk concentration divided by the boundary layer length scale. At sufficiently high bulk concentrations of surfactant, the surface concentration scale Γ_0' saturates as the interface is unable to accommodate any more surfactant. As the bulk concentration is increased beyond this point, the scale of the bulk diffusive rate continues to increase while that of the surface convective rate remains constant. The result is that molecular diffusion can easily compensate for or offset the accumulation created by the surface convection and thereby maintain (in the absence of a desorptive barrier) a uniform surface concentration and interfacial tension.

It is important to distinguish this regime of high bulk concentration from a contrasting regime of low bulk concentration where the characteristic equilibrium surface concentration is proportional to the bulk concentration. Since, in this regime, the surface concentration increases with that of the bulk, molecular diffusion cannot be made to outscale surface convection by increasing the bulk concentration. For this case, the ratio of the bulk diffusive and surface convective scales is described by a Peclet number ($\mathrm{Pe} = U'l'/D'$; U', l', and D' denote the fluid particle velocity and length scale, and D' is the bulk diffusion coefficient of surfactant). A uniform surface concentration is obtained (in the absence of desorption barriers) only at low Peclet numbers (large diffusion coefficients or small particle velocities). This case is not very practical since most fluid particle flows are at elevated Peclet number. Furthermore, the purposeful lowering of the particle velocity in an effort to reduce the Peclet number increases the magnitude of the Marangoni forces with respect to the viscous forces and this will act to decrease the surface convection in the neighborhood of the stagnation region.

Experimental support for the concept that, by increasing the bulk concentration of surfactant, bulk diffusion can be made to outscale surface convection and render (in the absence of desorption barriers) an interface uniformly populated with surfactant can be found in some of the results of the influence of surfactants on the propagation of longitudinal surface waves. As first studied by Lucassen and coworkers,[7,8] small amplitude longitudinal waves are created at the gas-liquid interface of a liquid film placed in a Langmuir trough by the in-surface periodic oscillations of opposing barriers positioned on the surface. The action of the barriers causes a periodic expansion and contraction ($\Delta A'/A'$) of the surface. A bulk soluble surfactant present in the liquid film adsorbs onto the surface, and the periodic area change causes the surfactant to, alternatively, desorb and diffuse away from the surface and adsorb and diffuse toward the surface. The periodic oscillation in the surface concentration ($\Delta\Gamma'$) causes an oscillation in the surface tension ($\Delta\gamma'$); the variation $\Delta\gamma'$ is related to the area oscillation $\Delta A'/A'$ by the complex surface elasticity parameter ϵ'; thus $\Delta\gamma' = \epsilon'\Delta A'/A'$, where $\epsilon' = \partial\gamma'/\partial \ln A'$. Lucassen and coworkers calculated ϵ' by measuring $\Delta\gamma'$ and $\Delta A'$. In particular, Lucassen and Giles[7] and Lucassen[8] present graphs of the modulus of ϵ' as a function of the bulk concentration of surfactant in the liquid pool for nonionic polethoxy surfactants ($C_{12}H_{25}E_3$, $C_{12}H_{25}E_6$, and $C_{14}H_{29}E_6$, where "E" denotes an ethoxy group —O—CH_2CH_2—, and each molecule terminates in a hydroxyl group) and an ionic surfactant, HDPS (hexadecyldimethylammoniopropanesulponate). These graphs indicate that although the modulus at first increases with C_∞', it goes through a maximum and then tends toward zero as the bulk concentration increases further. Lucassen and co-workers argue that these high concentration results indicate that the exchange kinetics and bulk diffusion are sufficiently fast so that the surface tension can remain uniform with oscillation ($\epsilon' = 0$). Two other points with respect to the longitudinal wave results of Lucassen and coworkers are important in the context of this study: First, the concentrations necessary to dissipate the elasticity increased with increasing frequency of oscillation; as the frequency increases, the rate of surface convection increases and larger bulk concentrations are necessary so that bulk diffusion can outscale convection. Second, the bulk concentrations necessary to eliminate the surface elasticity at high frequencies can be in excess of the critical micelle concentration (CMC). This fact gives rise to additional conditions that are necessary for surface mobility since the presence of micelles complicates the transport exchange process: Above the CMC most bulk surfactant is incorporated in micelles which most likely do not exchange with the surface. Consequently, in order for bulk monomer diffusion to outscale surface convection, it is now necessary to add the restrictions that the micellar–monomer exchange must be fast relative to surface convection, and that the *micellar* concentration be large enough so that the bulk diffusion of micelles is sufficiently fast relative to the convection. This study will also confirm that, for the surfactants used, concentrations above the CMC are necessary in order to remobilize a surface.

Although the experimental results of longitudinal wave theory indicate the likelihood that the surfactant retarded interface of a fluid particle can be made to be mobile if the bulk concentration is high enough and desorption barriers are absent, no studies have confirmed this, and the experiments reported herein are the first to attempt to do so. The fluid particle flow used to demonstrate remobilization is a three-phase periodic slug flow in a capillary. The flow consists of an alternating train of air and aqueous slugs drawn at a low capillary and Reynolds number through a Teflon tube of order 1 mm in diameter. The slugs ride on a thin cushion of a fluorocarbon oil film which is immiscible with the aqueous slug and which strongly wets the inside Teflon sur-

face of the tube wall in preference to gas and water. The thickness of the oil film is of the order of tens of microns and is controllable by the volumetric induction rate of oil. An illustration of the flow pattern in the frame moving with the train velocity U' is given in Fig. 1. Surfactant is dissolved in the aqueous slug phase and adsorbed onto the oil–water and air–water interfaces that form the periphery of the aqueous slug. Since the lubricating layer is so thin, a decrease in the interface mobility gives rise (at constant train velocity) to large retarding shear stresses in the oil layer, and these stresses increase the pressure drop required to drive the train flow. Therefore in this flow, the pressure drop is a sensitive indicator of the mobility of the interface, and remobilization at increasing bulk concentration is confirmed by measuring and following the reduction in the pressure drop. The surfactants used to verify the mobility conditions are the commercial nonionic polyethoxy surfactants, Triton X-100 [$CH_3C(CH_3)_2CH_2C(CH_3)_2C_6H_4E_nOH$] ($n$ between 9 and 10) and Brij-35 ($C_{12}H_{25}E_{23}OH$), which are soluble in the aqueous phase but not in the fluorocarbon oil. Related pendant drop tensiometry studies of these surfactants at the aqueous–air and aqueous–fluorocarbon oil interface, presented briefly in this study and more comprehensively in Lin *et al.*,[9] as well as the longitudinal wave theory results mentioned above by Lucassen and co-workers on similar but smaller chain polyethoxy surfactants, indicate that the desorption kinetics of these polyethoxy surfactants are sufficiently fast so as to be good candidates for remobilization. In addition, as a counter example, the protein bovine serum albumin (BSA) is used. The desorption kinetics of this surface adsorber is presumed slow because of denaturation of surface adsorbed protein, and the tendency of this protein to form desorption inhibiting multilayers at elevated bulk concentrations.

As has been mentioned, no direct experimental evidence, either for fluid particle flows in unbounded media or in confined geometries, has been presented which indicates that the retardation in surface velocity caused by surfactant adsorption can be relaxed under conditions of fast desorption kinetics and large bulk concentration. Certainly, the retarding influence of surfactant adsorption has been documented and studied for fluid particle flows. This is particularly true for the motion of fluid spheres in an infinite medium where theoretical efforts have exhaustively examined the regimes of slow kinetic or diffusive transport (the stagnant cap regime),[10–13] fast exchange[14–16] (uniform retardation), and the intermediate case of finite diffusive or kinetic transport[17–24] and the influence of surface viscosity.[25,26] Experimental studies have verified the retardation and have attempted reconciliation with the theoretical efforts.[27,28] With regard to slug flows in tubes, theoretical and experimental research has focused on the retardation due to surfactant adsorption for the case of a single slug moving in a continuous liquid phase containing a surfactant. In the remainder of this Introduction, this research is reviewed carefully below.

In the absence of surfactant, Bretherton[29] examined analytically the movement of a long gas slug in a capillary tube at low Reynolds and capillary numbers. He divided the

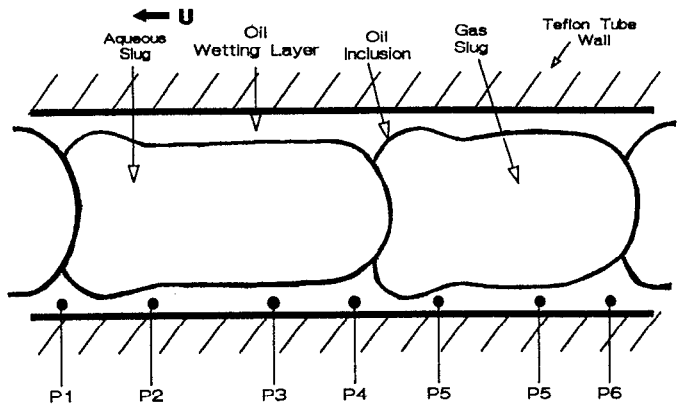

FIG. 1. Schematic of the three-phase slug flow regime illustrating the wetting layer, the oil inclusions, and the pressure distribution in a frame moving with the train velocity U'.

slug interface and surrounding fluid into five regions: (i) a center region where the wetting layer achieves a constant small value and no axial pressure drop occurs; (ii) two tip regions where only capillary forces are important and the shapes are to leading order sections of spheres; and (iii) two transition regions which bridge the tip and the constant wetting layer regions, and in which capillary and viscous forces are both important and the wetting layer fluid mechanics is described by the lubrication equations. By matching solutions in each of these regions in powers of the capillary number to the one-third power, Bretherton established that the constant wetting layer thickness and the pressure drop across the slug vary as the two-thirds power of the capillary number as this number tends to zero. While numerical solutions of the creeping flow equations for Bretherton's problem[30–34] have confirmed these asymptotic results, experimental attempts at verifying them, specifically the film thickness expression, have been met with mixed success since they usually indicate that the agreement is fair for Ca between 10^{-2} and 10^{-3}, but that the Bretherton expression increasingly underpredicts the film thickness as Ca decreases further.[29,35–39]

Theoretical studies of the influence of surfactant adsorption on the movement of fluid slugs began with the suggestion of Bretherton and Goldsmith and Mason[37] that the interface should be treated as tangentially immobile in order to account for the maximum influence of surfactant adsorption on the particle hydrodynamics. Using this assumption and retaining the stress-free asymptotic scalings at small capillary number, Bretherton demonstrated that the pressure drop across the slug and the constant film thickness surrounding the slug center increase by a factor of $2^{2/3}$. Bretherton's analysis is clearly inconsistent because the surface tension gradient needed to maintain tangential immobility is not accounted for in the normal stress balance.

Efforts at a more consistent low capillary number treat-

ment retaining the two-thirds scalings on the pressure and wetting layer thickness were undertaken by Herbolzheimer[40] and Ratulowski and Chang[41] for the leading edge problem of the motion of an infinite gas finger, and Hirasaki and Lawson[4] and Ginley and Radke[5] for finite gas slugs. Ratulowski and Chang examined the case in which the surfactant adsorption is asymptotically small in the capillary number, and they treat surfactant transport determined by bulk diffusion and sorption kinetics. Importantly, Ratulowski and Chang demonstrate that, for the particular case in which, relative to surface convection, sorption kinetics is fast enough to maintain bulk–sublayer equilibrium and bulk diffusion is slow enough so as to cause a depletion of surfactant in the wetting layer, the film thickness and the pressure increase from the Bretherton values. They further established that for sufficient adsorption, the elevation in the pressure and wetting layer thickness asymptote to values a factor $4^{2/3}$ larger than the clean surface values. Herbolzheimer also obtained these limiting values in a similar study.

Hirasaki and Lawson and Ginley and Radke examined for finite gas slugs the regime of uniform retardation controlled by sorption kinetics for order one elasticity (E) and Damköhler (D) numbers [$E = (\partial\gamma'/\partial\Gamma')(\Gamma_0'/\gamma_0')$] and $D = \alpha' R'\mu'/\gamma_0'$, where R is the tube radius and α is a molecular desorption rate; the subscript denotes values at equilibrium]. They all find that in the transition region, the deviation of the surfactant concentration from the equilibrium value is of order $Ca^{2/3}$, and they all derive essentially the same equation for the film thickness, surface velocity and surfactant distribution in that region. Hirasaki and Lawson simplify the transition region equations by assuming the film thickness is constant, and they present solutions for the pressure drop across the bubble in terms of this undetermined thickness and the ratio E/D. Their results indicate that as the ratio E/D increases from zero, the pressure drop increases from the Bretherton value. Ginley and Radke analyzed the regime of large Damköhler number, and match asymptotic expansions of the transition region equations to the tip equations. Their results again show an increase in the pressure drop as a function of E/D, but a decrease in the film thickness.

Experimentally, the retarding influence of surfactant adsorption on slug flows can first be inferred in the experimental study of Marchessault and Mason[36] who observed, under ostensibly clean surface conditions (although containing electrolyte), that the pressure drop across a bubble moving in a fluid-filled tube under low capillary and Reynolds number increased with the bubble length, and was larger than the Bretherton value. For an unretarded surface, since the wetting layer around the cylindrical region of the bubble is at rest, the pressure drop is only dependent on the curvatures at the front and back ends of the bubble. An increasing dependence on the bubble length, and the fact that the pressure drop was larger than the Bretherton value strongly indicate that the surface velocity of the long cylindrical interface is retarded. Marchessault and Mason realized that rigidification had taken place, but did not attribute it to inadvertent surfactant contamination. Experimental investigations by Delaunay[42] and Barthes-Biesel *et al.*,[43] intentionally adding the surfactant sodium dodecyl sulphate (SDS) to saline, confirmed the dependence on the bubble length, although both these studies show that the pressure drop asymptotes to a constant value with length. Direct visual evidence of retardation was obtained by Goldsmith and Mason:[37] Tracer particles placed in the film around the long cylindrical region were observed to move when surfactant was added, and were found to be stationary otherwise. Further recent studies by Hirasaki and Lawson[4] [using 1 wt % siponate DS-10 (a commercial sodium dodecyl benzene sulfonate) in water] and Ginley and Radke[5] (using 1 wt % SDS added to an equal weight percent water–glycerol mixture) also confirm experimentally that the pressure drop required to move gas slugs in the presence of surfactant adsorption is larger that the Bretherton value.

An outline of this paper is as follows. The study is divided into five sections. In Sec. II, the physicochemical conditions for surface mobility in the presence of surfactant adsorption are constructed (Sec. II A), and these conditions are recast in terms of the nondimensional groups of the three-phase flow (Sec. II B). In Sec. III, the equilibrium and sorptive kinetic properties of the surface adsorbers used in the study are described. In Sec. IV, the apparatus used to create the three-phase flow regime (Sec. IV A), and the manner in which the experiments were undertaken (Sec. IV B) are detailed. The results obtained verifying remobilization are detailed in Sec. V, and include the behavior in the absence of surfactant (Sec. V A), the data of the polyethoxy surfactants exhibiting remobilization (Sec. V B), and the protein results (Sec. V C). The paper concludes (Sec. VI) with a summary and a discussion of some of the implications of the ideas advanced.

II. PHYSICOCHEMICAL CRITERIA FOR SURFACE MOBILITY

A. Scaling arguments

Two transport processes, occurring in series, govern the exchange of surfactant molecules between the surface and the bulk. These are bulk diffusion and the kinetics of adsorption and desorption of surfactant from the sublayer underneath the surface onto the surface (termed here sorption kinetics). Consider as a simple example these processes as they occur in competition with surface convection at steady state on a nearly spherical fluid particle of length scale l' translating axisymmetrically at low Reynolds number with terminal velocity U' in an otherwise quiescent medium of infinite extent. For illustration, surfactant is assumed present in the continuous phase at concentration C_∞' far from the fluid particle. In the absence of motion the surface concentration in equilibrium with C_∞' is denoted as Γ_0'.

The rate at which surfactant is transported by surface convection through a perimeter of order l' oriented perpendicular to the surface flow is $O(\Gamma_0' U' l')$. To formulate and scale the kinetic exchange, factors which influence the sorption at high surface coverages must be accounted for, since remobilization is only realized under near saturation conditions. At high surface coverages the two most important factors that affect the exchange rate are (i) at high surface cov-

erages, the insertion and removal of a surfactant molecule from the monolayer requires that work must be done against an ever increasing surface pressure, and (ii) intermolecular interactions (repulsive or attractive) among adsorbed molecules can either raise or lower the energy of adsorption, and thereby affect the desorption rate. These effects are included, in a general manner, in the Frumkin kinetic equation where activation energies are dependent on the surface coverage:

$$Q' = \beta' \exp(-\nu_a' \Gamma'/R'T')C_s'(\Gamma_\infty' - \Gamma') - \alpha' \exp(-\nu_d' \Gamma'/R'T')\Gamma', \quad (1)$$

where Q' is the kinetic exchange rate for a surface coverage Γ' and sublayer concentration C_s'. In (1), α' and β' are desorptive and adsorptive kinetic rate constants, respectively, $R'T'$ denotes the gas constant multiplied by the absolute temperature, and Γ_∞' is the maximum packing concentration. In (1), the dependence of the activation energies on the surface coverage is assumed to be linear with coefficients $-\nu_d'$ and $-\nu_a'$ for desorption and adsorption, respectively; setting these constants equal to zero results in Langmuir kinetics. The surface concentration which is in equilibrium with the bulk concentration is obtained from (1) by setting Q' equal to zero and $C_s' = C_\infty'$; the result is

$$\Gamma_0'/\Gamma_\infty' = \phi = k/(e^{K\phi} + k), \quad (2)$$

where $K = (\nu_a' - \nu_d')\Gamma_\infty'/R'T'$ and $k = \beta' C_\infty'/\alpha'$. Note that when $\nu_a = \nu_d$, $K = 0$ and the Langmuir isotherm results from (2). The equilibrium equation of state $[\gamma_0'(\Gamma_0')]$, which follows from (2) and the use of the Gibbs–Duhem equation, is

$$\gamma'(\phi) = \gamma_c' + \Gamma_\infty' R'T'[\ln(1-\phi) - (K/2)\phi^2], \quad (3)$$

where γ_c' is the interfacial tension in the absence of surfactant.

To formulate a characteristic rate of desorption and compare this rate with the convective scale $(\Gamma_0' U' l')$ under the remobilization conditions of high bulk concentration $(k \gg 1)$ and near saturation coverage $[(\Gamma' - \Gamma_\infty')/\Gamma_\infty' = \Delta\Gamma \ll 1]$, consider the limit of $Ql'^2/(\Gamma_0' U' l')$ for $k \gg 1$ and $\Delta\Gamma \ll 1$. It can easily be demonstrated that to leading order in these inequalities, the ratio of the kinetic to the convective rate may be expressed as follows:

$$Ql'^2/(\Gamma_0' U' l') \approx -\nu[\exp(-K)\cdot k\cdot\Delta\Gamma + 1] \quad (4)$$

where $\nu = (\alpha' l'/U')\exp(-K_d)[K_d = (\Gamma_\infty' \nu_d)/R'T']$, and $k\Delta\Gamma$ is regarded to be of order one, in view of the above inequalities. Note that ν represents the ratio of the characteristic rate of desorption at high surface coverage to the rate of convection. The ratio of the Marangoni surface force ($\nabla_s'\gamma'$; ∇_s' denotes the dimensional surface gradient operator) to the scale of the shear stress exerted on the fluid surface of the particle $(\mu' U'/l')$ may be formulated exactly using (3) as $\mathrm{Ma}(\nabla_s\Delta\Gamma)[1/\Delta\Gamma - K(1+\Delta\Gamma)]$, where Ma (denoting the Marangoni number) is equal to $R'T'\Gamma_\infty'/(\mu' U')$ and μ' is the viscosity of the exterior fluid. In the limit $\Delta\Gamma \ll 1$, the ratio of Marangoni to viscous stresses may be expressed as follows:

$$\nabla_s'\gamma'/(\mu' U'/l') \approx \mathrm{Ma}(\nabla_s\Delta\Gamma)(1/\Delta\Gamma). \quad (5)$$

From Eq. (4) it can be concluded that when $\nu \gg 1$, the deviation from saturation, $\Delta\Gamma$, tends to a constant value $-(1/k)\exp(K)$; from (5) it is clear that the interface will remobilize since $\nabla_s\Delta\Gamma$ becomes zero.

The time scale for diffusion through the bulk is dependent upon the relationship between the convective and diffusive fluxes of surfactant in the bulk. A bulk Peclet number ordering these fluxes is defined as $U'l'/D'$, where D' is the bulk diffusivity of surfactant. Since the usual circumstance in mass transfer in liquids is the regime of large Peclet number, attention here will be restricted to this regime. When Pe is large, diffusion gradients normal to the surface which carry surfactant between the surface and the bulk exist in a small boundary layer of thickness δ'. Within this layer the diffusive flux normal to the surface is balanced by the convective flux in the direction along the surface. Clearly the scale of the diffusive flux to the surface of area $O(l'^2)$ is $O(l'^2 D' C_\infty'/\delta')$. The size of δ' is dependent upon the characteristics of the flow along the surface. The maximum flux develops when δ' is smallest, and this will be realized for a mobile interface for which δ' is of order $l'\,\mathrm{Pe}^{-1/2}$. Thus the scale of the maximum diffusive flux is $O[l'^2 D' C_\infty'/(l'\,\mathrm{Pe}^{-1/2})]$. Bulk gradients will not develop as long as the bulk concentration is large enough so that the surfactant diffuses quickly away from the surface; this will be the case when $[D' C_\infty' l'^2/(l'\,\mathrm{Pe}^{-1/2})]/(\Gamma_0' U' l') \gg 1$. The ratio Γ_0'/C_∞' appearing in the last inequality defines the adsorption depth h', the distance normal to the surface which contains (at equilibrium per unit area) as much surfactant as that adsorbed onto the surface.

We summarize the above arguments as follows: Under fixed values for D', U', and l', mobilization is realized if the surfactant's kinetics of desorption is intrinsically fast with respect to surface convection $(\nu \gg 1)$, and the bulk concentration is large enough so that h'/l' is sufficiently small to ensure that $(l'/h')\mathrm{Pe}^{-1/2} \gg 1$.

B. Nondimensional groups

In this subsection,the nondimensional groups that prescribe the three-phase flow are identified and the remobilization criteria developed above through scaling arguments are formulated explicitly in terms of the dimensionless groups related to the surfactant transport. An idealization of a repeating unit (a periodic cell) of the flow train is given in Fig. 1 in a frame in which the slugs are stationary. This idealization, referenced to a cylindrical coordinate system whose centerline is coincident with that of the tube, serves as the model for formulating the hydrodynamic and surfactant transport field equations and boundary conditions from which the nondimensional groups can be identified. The aqueous slug and the lubricating oil film are regarded as incompressible Newtonian fluids with, respectively, viscosities $\mu_{(a)}'$ and $\mu_{(o)}'$, and densities $\rho_{(a)}'$ and $\rho_{(o)}'$. Interfacial tensions *in the absence of surfactant* at the oil–aqueous, oil–gas and gas–aqueous interfaces are denoted by $\gamma_{(o/a)}'$, $\gamma_{(o/g)}'$ and $\gamma_{(g/a)}'$, respectively. The air slug is assumed to be incompressible and of negligible density and viscosity. Spatial, kinetic, and surfactant transport variables are scaled as fol-

lows: Spatial coordinates are scaled with the tube radius R', velocity vectors by U', pressure by the capillary scale $\gamma'_{(o/a)}/R'$, the bulk concentration by C'_∞ (the concentration in the reservoir from which the aqueous solution is drawn), and surface concentrations by the values in equilibrium with C'_∞, i.e., Γ'_0 and $\bar{\Gamma}'_0$, for, respectively, the oil–aqueous and aqueous–gas interfaces (the overbar denotes the aqueous–gas interface).

Nondimensionalization of the Navier–Stokes equations for the aqueous phase and the lubricating layer, and the surfactant transport equation in the aqueous phase (assuming only monomers are present diffusing according to Fick's law) results in the following dimensionless groups:

$$\kappa = \mu'_{(o)}/\mu'_{(a)},$$
$$\chi = \rho'_{(o)}/\rho'_{(a)},$$
$$\mathrm{Re} = R'U'\rho'_{(a)}/\mu'_{(a)},$$
$$\mathrm{Ca}_{(o/a)} = \mu'_{(o)}U'/\gamma'_{(o/a)},$$
$$\mathrm{Pe} = U'R'/D',$$

where D' is the bulk diffusion of surfactant in the aqueous slug, and Re, Ca, and Pe are, respectively, Reynolds, capillary, and Peclet numbers.

The kinematic constraints of continuity of velocity at the fluid interfaces, and at the inside surface of the tube do not add any additional dimensionless groups. The normal and tangential stress balances at the fluid interface must incorporate the variation in the surface tension resulting from the surfactant adsorption. The equilibrium equation of state that is used to described this dependence, and which follows from the Frumkin kinetic expression is given as Eq. (3); this equation is used here to describe the tension as a function of the nonequilibrium adsorption Γ' by replacing ϕ with Γ'/Γ'_∞. Using (3) the nondimensional normal and tangential stress balances at the fluid interfaces introduce the following additional dimensionless groups:

$$\mathrm{Bo} = (\rho'_{(o)} - \rho'_{(g)})g'R'^2/(\gamma'_{(o/a)}),$$
$$\mathrm{Ca}_{(o/g)} = \mu'_{(o)}U'/\gamma'_{(o/g)},$$
$$\mathrm{Ca}_{(a/g)} = \mu'_{(a)}U'/\gamma'_{(a/g)},$$
$$k = \beta'C'_\infty/\alpha' \quad (\bar{k} = \bar{\beta}'C'_\infty/\bar{\alpha}'),$$
$$K = (\nu'_a - \nu'_d)\Gamma'_\infty/R'T' \quad [\bar{K} = (\bar{\nu}'_a - \bar{\nu}'_d)\bar{\Gamma}'_\infty/R'T'],$$
$$\mathrm{Ma} = R'T'\Gamma'_\infty/(\mu'_{(o)}U') \quad [\overline{\mathrm{Ma}} = R'T'\bar{\Gamma}'_\infty/(\mu'_{(o)}U')],$$

where g' is the gravitational acceleration constant and the overbar in the surfactant dimensionless groups differentiates the aqueous–gas interface from that of the aqueous–oil interface.

The crucial equations which describe the remobilization effect are the surfactant transport equations at the oil–aqueous interface. These equations in nondimensional form are detailed explicitly here for the oil–aqueous interface:

$$\nabla_s\cdot(\Gamma\mathbf{v}) = [\mathrm{Pe}(h'/R')]^{-1}\mathbf{n}\cdot\nabla C = [\Phi k/(\phi)]\mathbf{n}\cdot\nabla C, \tag{6}$$

$$\nabla_s(\Gamma\mathbf{v}) = \nu^*\{\exp[-K_d(\phi\Gamma - 1)]\} \times [kC\cdot e^{-K\phi\Gamma}/\phi - \Gamma(kC\cdot e^{-K\phi\Gamma} + 1)], \tag{7}$$

where $\mathbf{n}$ denotes the unit vector to the oil–aqueous interface directed into the aqueous phase, $\mathbf{v}$ denotes the surface velocity vector, and C the nondimensional surface concentration;

$$h'/R' = \Gamma'_0/(C'_\infty R') = k^{-1}\phi(k)(\beta'\Gamma'_\infty/R'\alpha'),$$
$$\Phi = (D'\alpha')/(\beta'U'\Gamma'_\infty),$$
$$K_d = \nu'_d\Gamma'_\infty/R'T',$$
$$\nu^* = \alpha'[\exp(-K_d)]R'/U',$$

where $\phi(k)$ is defined implicitly by Eq. (2). Note that the term $[\mathrm{Pe}(h'/R')]^{-1}$ in Eq. (6) is written in terms of a nondimensional group that is independent of C'_∞ and the k (or C'_∞) dependent group $k/\phi(k)$. Therefore from (6) and (7) three additional dimensionless groups are introduced, Φ, ν^*, which is analogous to the ν defined generally in the scaling arguments of Sec. II A, and K_d. Note also that in the formulation of the surfactant mass conservation equations on the slug interface [Eqs. (6) and (7)], surface diffusion has been neglected since in the regimes of interest here, surface Peclet numbers ($U'R'/D'_s$) are very large [$O(10^5)$] and therefore surface convection dominates surface diffusion. Note finally that parameters analogous to h'/R', ν^*, and K_d arise when the surfactant mass balance equations are formulated at the aqueous–gas interface.

The specification of the dimensionless groups is completed with the formulation of integral constraints which set the size of the gas and aqueous slugs to the values formed in the experimental apparatus, and equate the volumetric flow rate of oil in a laboratory frame to the rate at which oil is introduced by an infusion pump. The slug constraints are straightforward and introduce the variables λ, the ratio of the characteristic axial length of the repeating unit of the flow train to the tube radius and ϵ, the void fraction of gas in the repeating unit. These variables are defined below:

$$\lambda R' = (V'_{(g)} + V'_{(a)})/(\pi R'^2),$$
$$\epsilon = V'_{(g)}/(V'_{(g)} + V'_{(a)}),$$

where $V'_{(g)}$ and $V'_{(a)}$ denote the volumes of the gas and aqueous slugs, respectively. The volumetric flow rate of oil in the train-fixed reference frame is termed the leak rate q'_{lk}, and is in a direction opposite to the train flow. This rate is given dimensionally by $q'_{lk} = \int_{\partial V'_c}\mathbf{n}\cdot\bar{\mathbf{v}}'\,da'$, where $\partial V'_c$ is any cross-sectional area perpendicular to the tube axis and through which oil flows, and $\mathbf{n}$ is the normal to that surface directed opposite to the train flow. The volumetric flow rate in the laboratory fixed frame (i.e., the oil pump infusion rate) is denoted by q'_{oil} and is easily shown to be equal to $-q'_{lk}$ added to the volume of oil in the unit cell ($V'_{(o)}$) divided by the time which transpires for a unit cell to pass a fixed point in the laboratory frame (Υ'). Nondimensionalizing the expression for q'_{oil} by the nominal aqueous flow rate ($\pi R'^2U'$) yields the final dimensionless group $\Omega = q'_{\mathrm{oil}}/(\pi R'^2U')$.

From the arguments presented in Sec. II A, it is clear that the central equations with regard to the surfactant influence on the surface mobility of the aqueous–oil interface (the only one which significantly affects the pressure drop) are Eqs. (6) and (7). In the limit in which ν^* becomes large,

the sublayer and the surface are in equilibrium. In addition, as $[\mathrm{Pe}(h'/R')]^{-1}$ becomes large with increasing bulk concentration, the diffusive flux to the surface ($\mathbf{n}\cdot\nabla C$) tends to zero and the bulk concentration becomes uniform. This fact, taken together with the sorption equilibrium, ensures that the surface concentration is uniform and the surface is mobile. However, these conditions are unnecessarily conservative since the characteristic length scale for surface convection is $O[R'\lambda(1-\epsilon)]$ rather than order (R') and that for bulk diffusion it is of order ($R'\,\mathrm{Pe}^{-1/2}$) owing to the diffusion boundary layer rather than R'. Using these more representative scalings for the slug flow, the conditions for mobility become (i) $\nu=\alpha'\exp(-K_d)R'\lambda(1-\epsilon)/U'\gg 1$ and (ii) $(R'/h')\mathrm{Pe}^{-1/2}=[\Phi k/\phi(k)]\mathrm{Pe}^{1/2}\gg 1$.

III. EQUILIBRIUM AND SORPTION KINETIC PROPERTIES OF THE SURFACE ADSORBERS

The surface adsorbers used in this study are the protein BSA and the polyethoxy surfactants Triton X-100 and Brij-35. The equilibrium interfacial properties of aqueous solutions of BSA have been extensively studied at both the air–water and water–oil (n-decane) interfaces by Graham and Phillips[44] using a Wilhelmy plate technique to measure surface tensions, and radioactive labeling of the protein molecule to obtain an independent measure of the surface adsorption. At both interfaces, the results of Graham and Phillips show evidence of multilayer adsorption of bulk concentrations exceeding 1.5×10^{-10} mole/cm^3 because above this value surface adsorption was found to continue to increase while the surface tension remained constant. Guzman *et al.*[45] have used the Graham and Phillips data at the air–water interface to successfully construct a two layer adsorption isotherm with the primary, surface tension lowering layer, described by a Frumkin model [Eq. (2)]. Their results for the model constants Γ'_∞, β'/α', and K are listed in Table I.

More importantly, MacRitchie and Alexander[46,47] and Graham and Phillips[44] studied the adsorption kinetics of BSA. Each of these studies considered the desorption term in (1) to be negligible because of surface denaturation (see also Ter Minassian-Saraga[48]), and therefore regarded this term as playing no role in accounting for the adsorption behavior. Experimentally, both studies found that when BSA adsorbs onto a freshly created interface, there was an initial period of adsorption where the rate varies as the minus one-half power of the time (t) from interface exposure. Since this result represents the solution for diffusion controlled mass transfer at zero sublayer concentration, these studies concluded that, at low surface coverages, no adsorption barrier exists. After the initial period, the adsorption rate decelerated with increasing surface coverage, and large departures from the $t^{-1/2}$ behavior were observed. This effect was attributed to the fact that at these advanced times when the surface coverage and therefore the surface pressure is high, more work must be done to insert the protein molecule into the already existing layer. This energy prerequisite represents the activation energy for adsorption, and is described in Eq. (1) by the term $\exp(-\nu'_a\Gamma'/R'T')$.

MacRitchie and Alexander[47] attempted to quantify the role of higher surface pressures on decelerating adsorption by undertaking unsteady experiments at constant surface pressure. For adsorption, MacRitchie and Alexander formulated the following equation which is similar to (1) except that it neglects any desorption or saturation:

$$Q'=\bar{\beta}'C'_\infty\exp(-\pi'\Delta A'/R'T'),$$

where π' is the surface pressure and $\Delta A'$ is the area, per molecule, that is necessary to clear in order to insert the protein molecule into the monolayer. Experiments were undertaken at 4.5×10^{-10} mole/cm^3, a relatively high concentration where the surface pressure is at its maximal value of 18 dyn/cm and the primary layer surface concentration is near the saturation value of 4.6×10^{-12} mole/cm^2 (cf. Table I). By measuring rates of adsorption at different imposed surface pressures and using a linear regression, MacRitchie and Alexander obtained a value of order 10^6 cm^3/(mole sec) for β' ($\bar{\beta}'=\beta'\,\Gamma'_\infty$). From knowledge of the equilibrium value for $\beta'/\alpha'=7.35\times10^{11}$ cm^3/mole (cf. Table I), α' can be estimated to be of order 10^{-6} sec^{-1} and ν $[=\alpha R'\lambda(1-\epsilon)/U']$ to be of order 10^{-5} using the data of Table II (see below). Therefore, it is expected (and will be shown to be the case, cf. Sec. V C) that under the conditions of the experiment, aqueous slug interfaces with adsorbed BSA should not become mobile at high bulk concentrations.

The equilibrium and sorption kinetic properties of aqueous solutions of the polyethoxy surfactants against air and the fluorocarbon oil were measured using pendant drop tensiometry enhanced by video image digitization. In this

TABLE I. Equilibrium adsorption properties.

	Γ'_∞ (mole/cm^2)	β'/α' (cm^3/mole)	K	C_{CMC} (mole/cm^3)	γ_{CMC}/γ_c (dyn/cm)
Air/TRX-100[a] (L)	2.91×10^{-10}	1.51×10^{9}			
(F)	3.20×10^{-10}	3.22×10^{9}	2.52	2.3×10^{-7}	30.4/72.5
Oil/TRX-100[a]	1.96×10^{-10}	8.47×10^{10}		4.2×10^{-7}	9.2/59.5
Oil/Brij-35[a]	1.40×10^{-10}	3.23×10^{12}		3.7×10^{-8}	16.8/59.5
Air/BSA[b]	4.64×10^{-12}	7.35×10^{11}	1.117		55.0/72.5

(F) Frumkin isotherm; (L) Langmuir isotherm.

[a] Data obtained from pendant drop tensiometry as part of this study; for details see Lin *et al.*[9]

[b] Data obtained from Graham and Phillips;[44] Frumkin equilibrium constants obtained from Guzman *et al.*[45]

TABLE II. Surfactant-independent dimensionless groups.

Dimensionless group	Clean water TRX-100/Brij-35 0.097 cm i.d.	Clean water and TRX-100 0.155 cm i.d.	BSA 0.155 cm i.d.
Void fraction (ϵ)	0.43	0.42	0.42
Aspect ratio (λ)	81.5	81.5	85.0
Viscosity ratio[a] (κ)	5.9	5.9	5.9
Oil–aqueous flow rate ratio (Ω)	3.3×10^{-3}	3.2×10^{-3}	3.3×10^{-3}
Oil–aqueous capillary number	1.02×10^{-3}	1.02×10^{-3}	1.02×10^{-3}
Oil–gas capillary number	3.80×10^{-3}	3.80×10^{-3}	3.80×10^{-3}
Aqueous–gas capillary number	1.42×10^{-4}	1.42×10^{-4}	1.42×10^{-4}
Aqueous– oil Bond number[b]	3.6×10^{-2}	9.0×10^{-2}	9.0×10^{-2}

[a] Obtained using a value of 0.89 cP for the viscosity of water and 5.26 cP for that of FC-43,[57] both at 25 °C.
[b] Obtained using a value of 1.88 g/cm^3 for the density of the fluorocarbon oil at 25 °C.[57]

technique an air bubble or oil droplet is formed at the tip of a stainless steel needle that is immersed in the surfactant solution. The formation time is of the order of a few seconds for an oil drop, and a second or two for a gas bubble. After creation, surfactant diffuses toward, and adsorbs onto, the freshly created interface where it lowers the interfacial tension until equilibrium is achieved. The dynamic interfacial tension is measured by first imaging a silhouette of the drop onto a video camera, and then digitizing at known time intervals the image in order to determine the shape of the drop surface. From the experimentally determined shape, the surface tension can be computed by minimizing the difference between the experimental construct and one determined by numerical integration of the Young–Laplace equation. The use of video imaging and sequential digitization results in a more accurate determination of the surface tension than the classical pendant drop technique where photographs of the pendant drop are used to measure an aspect ratio, and the surface tension is determined from that ratio through a look-up table. An introduction to this technique is provided in several papers.[49] This particular application is part of a larger study of the sorption kinetics of surfactants by Lin *et al.*,[9] and the details of the construction of the apparatus, the determination of the surface tension, and the solution of the diffusion-limited and mixed diffusion-kinetic surfactant mass transfer problems are described in that study.

The equilibrium surface tensions of aqueous solutions of Triton X-100 against air and fluorocarbon oil, and aqueous solutions of Brij-35 against oil are shown in Fig. 2 as a function of the bulk concentration of surfactant. Each of these three systems exhibit CMC behavior occurring at 2.3×10^{-7} mole/cm^3 for Triton X-100 against air, and 4.2×10^{-7} mole/cm^3 and 3.7×10^{-8} mole/cm^3 for, respectively, oil–water systems of Triton X-100 and Brij-35. Efforts at modeling these curves below the CMC using the $\gamma' - \ln C'$ dependence, which follows from the Frumkin isotherm [cf. Eqs. (2) and (3)], gave the following results. For the Triton X-100–air system, much better congruence was achieved with K positive and not equal to zero, then when $K = 0$ was used [compare the solid (Frumkin) and dashed (Langmuir) lines]. In the case of the oil–water systems, the Langmuir isotherm ($K = 0$; $\nu_a = \nu_a$) proved sufficient. The model constants for each of the theoretical constructs are detailed in Table I.

Sample relaxation data for aqueous solutions of Triton X-100 at the air–water and oil–water interfaces are given in Fig. 3 and 4 at concentrations $C'_\infty = 9.89\times10^{-9}$ mole/cm^3 and 1.55×10^{-8} mole/cm^3, respectively. To examine quantitatively the relaxation, consider first that the process is diffusion limited. Numerical solutions of the bulk diffusion equations and the adsorption isotherm (Frumkin for the aqueous–air surface, Langmuir for the aqueous–oil interface) can be used to generate relaxation curves once a value of the diffusion coefficient is selected. The results are shown

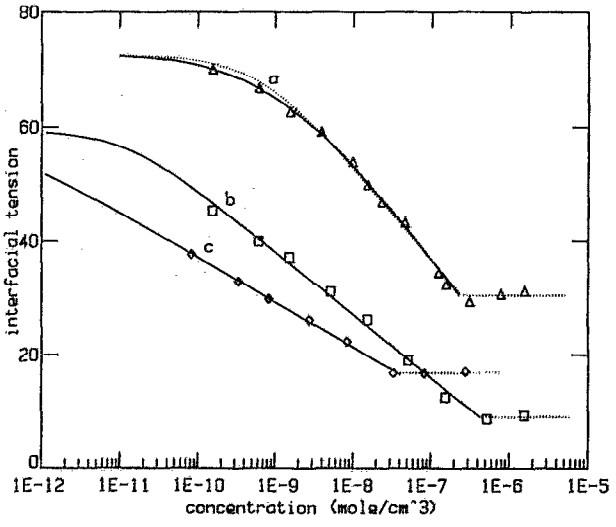

FIG. 2. Interfacial tensions of Triton X-100 aqueous solutions at the air–water (a) and oil–water (b) interfaces, and of Brij-35 aqueous solutions at the oil–water interface (c) as obtained from pendant drop tensiometry. The lines through the data are the predicted surface tensions using the Frumkin (solid) and Langmuir (dotted) isotherms for the air–water surface and the Langmuir isotherm for the oil–water interfaces [(b) and (c)].

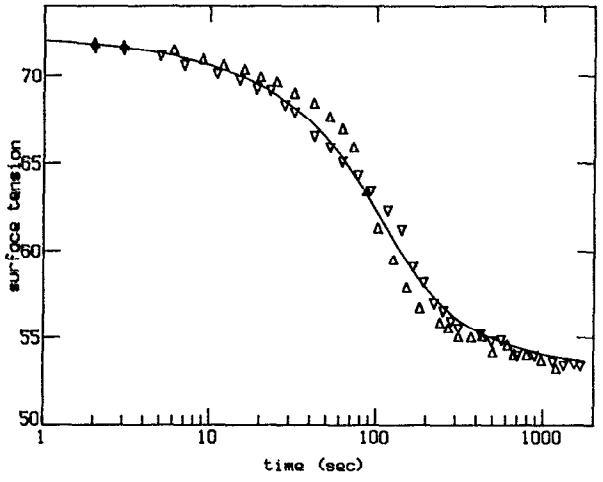

FIG. 3. Experimental data for the relaxation of the surface tension of pendant air bubbles in Triton X-100 solutions as a function of nondimensional time, and the numerical solution of the diffusion-limited transport equations (using the Frumkin isotherm, and associated equation of state), all for a bulk concentration of 9.89×10^{-9} mole/cm^3 and a diffusion coefficient of 2.6×10^{-6} cm^2/sec.

as the solid line in Fig. 3 and the dotted line in Fig. 4, each for a value of the diffusion coefficient of 2.6×10^{-6} cm^2 sec^{-1}. The agreement is fairly good, and it can therefore be concluded that the sorption kinetics is fast. To quantify just how fast, consider the oil–water interface: Plotted in Fig. 4 alongside the diffusion-limited curve are the relaxations for different values of β' assuming Langmuir kinetics. By comparing the mixed and diffusion-limited models it is clear that β' is at least as large as 10^8 cm^3/(mole sec), and this translates to a lower bound value for α' of 10^{-3} sec^{-1} and $\nu\,[=\alpha' R'\lambda(1-\epsilon)/U']$ of 10^{-2} using the data of Table II (to be discussed below). Values of β' larger than 10^8 cm^3/(mole sec) are of course consistent with the relaxation in Fig. 4, but no larger lower bound can be inferred because of the closeness, for $\beta' > 10^8$ cm^3/(mole sec), of the mixed curves to each other an to the diffusion-limited curve. Since values of ν much larger than one are a necessary prerequisite for the observed remobilization of Triton X-100, the values of β' are presumably larger than the lower bound established here.

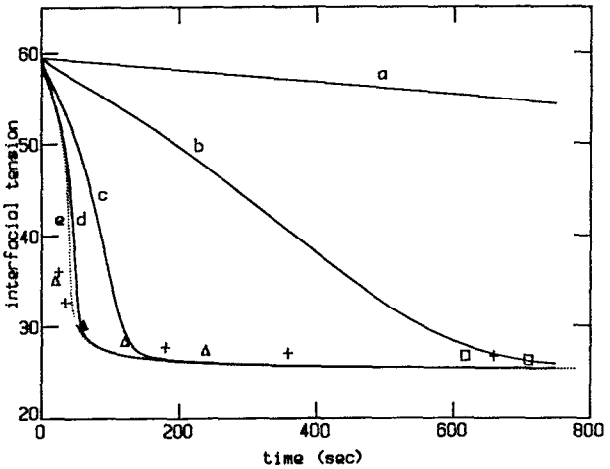

FIG. 4. Experimental data for the relaxation in interfacial tension of oil drops in aqueous Triton X-100 solutions for a bulk concentration of 1.55×10^{-8} mole/cm^3. Shown alongside the data are the numerical simulations of the diffusion-limited (dotted line, labeled e) and mixed kinetic-diffusion (solid lines, labeled a–d) surfactant mass transport equations for a diffusion coefficient of 2.6×10^{-6} cm^2/sec. The mixed equation numerical solutions are for values of β' equal to: (a) 10^5, (b) 10^6, (c) 10^7, and (d) 10^8 cm^3/mole sec).

Joos and co-workers have also studied the adsorption kinetics of Triton X-100 at the air–water and oil(hexane)–water interface using the drop volume, oscillating jet, and flowing film methods and at the oil(hexane)–water interface using the drop volume technique.[50–52] They find that the equilibrium properties for Triton X-100 at both interfaces can be described by Langmuir isotherms with constants in agreement with those tabulated in Table I. Joos and co-workers also find no evidence of sorption kinetic barriers in the dynamic surface tension relaxations measured, and they infer a diffusion coefficient of approximately 2×10^{-6} cm^3/sec in agreement with this study.

The kinetics of the Brij-35 surfactant has not been measured by pendant drop tensiometry. However, its sorption kinetics is assumed to be similar to that of Triton X-100 since the molecular structure of the Brij-35 molecule resembles that of Triton X-100 with the only differences being the number of ethoxy groups (23 as opposed to 9), and a more slender nonpolar hydrocarbon part. Studies by Joos and co-workers on a similarly structured polyethoxy surfactant with approximately the same number of ethoxy groups (Brij-58) and the same hydrocarbon part at the air–water and oil(hexane)–water interfaces using the drop volume, reversed funnel, and Langmuir trough compression techniques,[52,53] show no evidence of kinetic barriers and a diffusion coefficient approximately equal to that of Triton X-100.

Note finally that the desorption estimates obtained from the data of MacRitchie and Alexander for BSA and Triton X-100 from Fig. 4 do not account for high surface coverage decelerating effects on the desorption caused by cohesive energies among adsorbed species or the work required to be done against the surface pressure to allow a molecule to desorb. For both the protein and Triton X-100, large cohesive energies between the hydrophobic regions of the molecules are not expected because the molecular geometry of these regions are not long and slender, and therefore do not promote favorable van der Waals interactions. This assertion is also supported by the fact that at the air–water interface, the parameter K was found to be positive for both BSA and Triton X-100, indicating repulsion rather than attraction of the adsorbed species. Also note that at an oil–water interface, all interactions of adsorbed species are modulated by molecules of the oil which themselves interact with the hydrophobic chains of the adsorbed molecules; this may explain why for Triton X-100 adsorbing at the oil–water inter-

face, K is equal to zero and the saturation coverage is less than that at the air interface (cf. Table I). However, other surface adsorbers such as the n-alcohols octanol and decanol do demonstrate large cohesive energies ($K<0$), and if such molecules are considered in the context of remobilization, cohesive lowering of the desorption rate is a factor that should be taken into account. Note also that the work required against the surface pressure was also not taken into account. The data of MacRitchie and Alexander indicate a value for $\Delta A'$ of 135 Å^2, and therefore the decelerating factor $[\exp(-\pi'\Delta A'/R'T')]$ is of order 10^{-2}–10^{-3} for Π in the range of 10–20 dyn/cm. Thus the parameter ν can be expected to be a few orders of magnitude less than the 10^{-5} estimated, and these smaller values are certainly consistent with the experimental results. With regard to Triton X-100 and Brij-35, since these molecules are much smaller than the protein, the work required against the surface pressure to desorb a molecule is not assumed to be significant.

IV. THREE-PHASE SLUG FLOW

A. Apparatus design

The apparatus which creates the segmented flow is detailed in Fig. 5. A three-way miniature solenoid valve (Lee Co.) is configured so as to draw either air or aqueous surfactant solution. The solenoid valve is attached to a piece of glass tubing (i.d. = 1.7 mm). Along the length of glass tubing two IR emitter–detector pairs are located a known distance from the solenoid valve. The IR emitter–detector pairs are configured through a relay circuit which allows them to control the solenoid valve. The glass tube is initially filled with aqueous surfactant solution. A small air slug is formed and drawn through the length of tubing. When the aqueous–air interface passes the first IR emitter–detector pair the solenoid begins to draw in air. When the same aqueous–air interface passes the second detector the solenoid draws aqueous solution. The length of an air slug is therefore determined by the distance between the two detectors; the length of an air–aqueous slug pair is determined by the distance between the solenoid valve and the first detector. This manner of creating the segmented flow is reproducible and creates a periodic flow pattern independent of flow velocity. The glass tubing is attached to a T section through which fluorocarbon oil (FC43, 3M) is injected at a known flow rate by an infusion pump (Sage Instruments). The downstream end of the T section is attached to the experimental test section, which consists of a length of Teflon tubing. Since the fluorocarbon oil which was used preferentially wets Teflon, the oil injected by the infusion pump at the T section will wet the Teflon tube wall, forming an annular oil film and establishing the three-phase flow pattern.

The experimental test section (Fig. 6) to which the segmented flow apparatus is attached consists of a length of Teflon tubing whose average inner diameter is measured by weighing the length, first empty and then filled with water. The tubing, which is oriented horizontally, is attached at the extreme downstream end to a peristaltic pump (LKB Productor Microperpex pump). Velocity measurements are made for each unit cell as it passes through the test section by

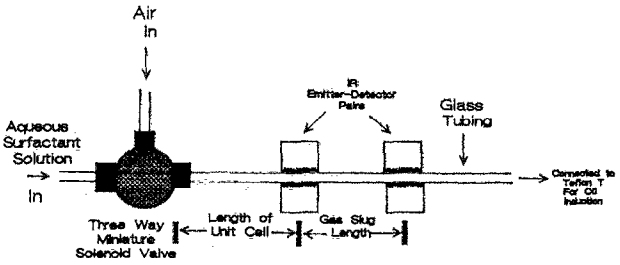

FIG. 5. Schematic of the solenoid network and relay system employed to create the periodic flow regime.

two IR emitter–detector pairs located at either end of the test section. Also located at the upstream and downstream ends of the system are two pressure taps. These are simply T sections that are attached to fluid filled tubes which lead to either side of a diaphragm-type differential pressure transducer (Validyne). Both the IR emitter–detector pairs and the pressure transducer are attached to an A/D card (Data Translation DT2805); the pressure drop and the average velocity over the length of test section are monitored continuously during a run.

B. Materials and methods

The surface adsorbers which were dissolved in the aqueous phase were Triton X-100 and Brij-35, obtained from Aldrich Chemical Co.; bovine serum albumin, obtained from Sigma Co.; and FC-43 fluorocarbon oil from 3M. Both the surfactant and protein were used without modification. Solutions of BSA were made in a buffer solution of sodium phosphate dibasic and potassium phosphate monobasic with a pH of 7.0 and an ionic strength of 0.16. Hydrion dry buffer was used as obtained from Micro Essential Laboratory; no preservative was added, and the solutions were made fresh daily. The water with which the

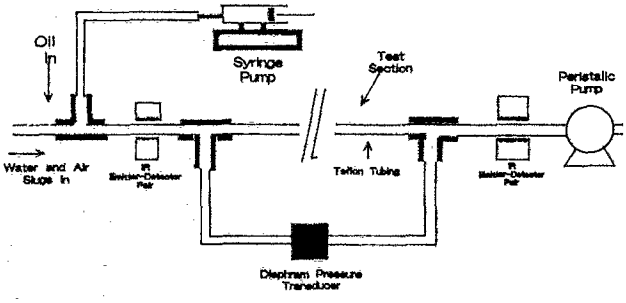

FIG. 6. Schematic of the experimental test section over which the pressure drop required to draw the three-phase slug flow through the Teflon capillary tube and the slug velocity is measured.

aqueous solutions were made was purified via a Millipore water purification system; the Teflon tubing which serves as the test section was obtained from Alltech Associates (FEP, nominal i.d. of 1.5 and 1.0 mm). All experiments were undertaken at 25 °C ($\pm$ 2 °C).

A series of runs were undertaken in which solutions of varying concentration of surfactant are used to form the aqueous slug in the three-phase slug flow geometry. The pressure drop required to drive the flow at each concentration was measured over the course of a run. Each day the first run was one in which the aqueous slug consisted of pure water. The pressure drop for this run was used as a benchmark and provided a check for excessive impurities in the system. Subsequent runs were undertaken in order of increasing surfactant concentration. At the end of each day the tubing was flushed out for several hours using pure water.

The experiments were undertaken in the following manner. Three-phase flow is established in the system using a surfactant solution at some bulk concentration. The pressure drop over the test section, $\Delta P'$ is monitored until it attains a steady value at a train velocity U' of 1.15 cm/sec; U' and $\Delta P'$ are then recorded over a 45–60 min. time period, with the $\Delta P'$ at the time that each air slug passes the second velocity detector being recorded along with that slug's average velocity over the test section. Between runs the system is flushed out for several hours with purified water if the following run is to be one with a lower concentration of surfactant than its predecessor, otherwise the higher concentration solution was used without washing.

The dimensionless groups can be divided into two classes, those that are related to the effect of surfactant, and those that are independent of surfactant effects. Those in the surfactant-independent group are ϵ, λ, Ω, κ, Bo and the capillary numbers. The values at which these groups are held fixed in the experiments reported herein are tabulated in Table II. The tabulated viscosity ratio was obtained from the literature value of the fluorocarbon oil at 25 °C and with the surfactant and protein solutions assumed to have the viscosity of pure water at 25 °C. Capillary numbers were computed using the interfacial tensions of the aqueous–oil and aqueous–air interfaces as obtained from the pendant drop tensiometry experiments of Sec. III. (Note, however, that these experiments were undertaken at 22.5 °C $\pm$ 0.5 °C.) The viscosity ratio κ remains constant as all experiments are undertaken using the same fluorocarbon oil. The ratio of oil to aqueous flow rates within the system, Ω, is held fixed by fixing the rate at which oil is introduced into the system by the infusion pump, U' being held constant for all experiments reported herein. The void fraction ϵ and the aspect ratio λ are established as follows. The length of a unit cell in the test section is fixed by fixing the distance between the solenoid valve and the first detector at the extreme upstream end of the apparatus. This length is checked by making sure that the correct number of unit cells appear between the IR emitter–detectors that monitor the average velocity over the test section. The void fraction is established by measuring the volume of liquid in several hundred unit cells, and adjusting the distance between the two detectors at the extreme upstream end of the system until the desired void fraction is attained. All of these adjustments are made before fluorocarbon oil is introduced to the system, as ϵ and λ are defined to be the void fraction and aspect ratio in the absence of an oil film.

The surfactant-dependent groups are ν^*, Φ, K, K_d, Ma, Pe, and k. For each surfactant Φ, Ma, K, K_d, and Pe do not change with C'_∞ (these constant values are reported in Table III with the exception of K which is given in Table I). The parameter k, however, increases with concentration; to verify remobilization, it is necessary to check that the pressure drops return to clean surface values as the bulk concentration and, in particular, $(R'/h')\mathrm{Pe}^{-1/2}$ $(= [\Phi k/\phi(k)]\mathrm{Pe}^{1/2})$ becomes large.

V. RESULTS AND DISCUSSION

A. Clean surface results

1. Interfacial shapes

The interfacial shape assumed by a single long gas slug suspended in Poiseuille flow at low Reynolds number in a capillary tube has been detailed asymptotically at low capillary numbers by Bretherton. For small Ca, the leading edge of the slug is nearly hemispherical in shape, with a radius of curvature slightly smaller than the tube radius. This hemispherical region is attached via a transition region to a long cylindrical region of nearly constant wetting layer thickness which, in the frame moving with the bubble, moves uniformly with the slug velocity. This cylindrical region, in turn, is

TABLE III. Surfactant-dependent dimensionless groups.[a]

Dimensionless group	Triton X-100 0.097 cm i.d.	Brij-35 0.097 cm i.d.	TRX-100 0.155 cm i.d.	BSA 0.155 cm i.d.
Peclet number (Pe)	2.2×10^{4}	2.2×10^{4}	3.4×10^{4}	1.5×10^{5}
Marangoni number (Ma)	8.0×10^{1}	5.7×10^{1}	8.0×10^{1}	1.9
Φ[b]	1.4×10^{-7}	5.0×10^{-9}	1.4×10^{-7}	1.5×10^{-7}

[a] Dimensionless groups evaluated at the aqueous–oil interface, with the exception of the BSA for which aqueous–gas data are used.
[b] Obtained using a value of 6.0×10^{-7} cm^2/sec for D' of BSA (MacRitchie and Alexander[46]) and 2.6×10^{-6} cm^2/sec for Triton X-100 and Brij-35 (cf. Sec. III).

pinched-in in the region just before the trailing end of the slug. The trailing edge is distended in the direction opposite to the flow and has a radius of curvature that is greater than the tube radius. The pinching-in of the slug at the trailing end is caused by the applied pressure gradient, and is necessary to set the fluid in the back of the slug in motion.

In the connecting slug flow regime of this study, it is expected that the oil wetting layer interfacial shape should be similar, again exhibiting pinching-in of the trailing slug ends. However, the aqueous–air interfaces which constitute the back and the front ends of the gas and aqueous slugs should both be distended in the direction of the flow. (The presumed interfacial profiles are illustrated in Fig. 1.) The reason for the assumed bending of the aqueous–air interfaces in the flow direction is that the curvature of the leading end of a slug is always slightly larger than $2/R'$ while that of a trailing end is slightly less than $2/R'$. Since in the train flow both the fluid in the back of the leading edge of one slug and in front of the trailing edge of the attached slug are related to the pressure in the oil inclusion by the curvature, the pressure of the fluid behind the leading edge is larger than that in front of the trailing edge.

Photographs of magnified images of the flow confirm some of these expectations. In Figs. 7(a) and 7(b) photographs of the leading and trailing ends of an aqueous slug in three-phase slug flow are shown in the 0.155 cm i.d. tube at 30× magnification for clean surface conditions and a parameter range for the dimensionless groups as given in Table II. In these photographs, the gas slug appears dark and the aqueous segment appears clear. The oil around the liquid segment appears as a dark line, while the oil in the three-phase contact region forms an inclusion that is shaded light grey. Note that the leading edge of the aqueous slug depicted in Fig. 7(a) appears nearly hemispherical except where the aqueous–air slugs adjoin. Importantly, the pinching-in of the trailing edge of the aqueous slug is discernible. It is not clear whether or not the gas slug also flares out at its trailing end because of the similar shading of the gas slug and its surrounding oil film. Also the exact details of the aqueous–air interface configuration are not clear from the photographs.

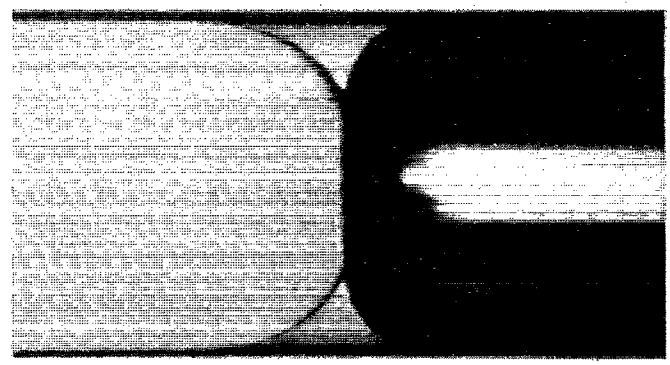

(a)

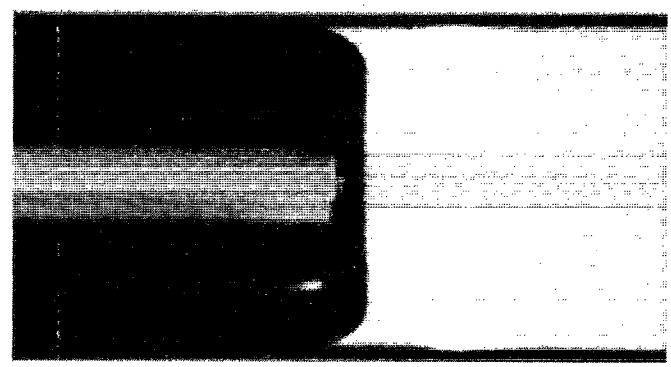

(b)

FIG. 7. (a) Photograph at 30× magnification of the slug flow for clean interface conditions in the 0.155 i.d. tubing. The plate shows the leading edge of the aqueous slug (light area), the trailing edge of the gas slug (dark shading), the three-phase contact ring, and the oil inclusion surrounding this ring. (b) Photograph of the trailing edge of the aqueous slug under the same conditions as (a) showing explicitly the pinching-in of the wetting layer film at the rear of the aqueous slug.

2. *Clean interface pressure drop results*

All of the pressure drop data presented in this and the remaining subsections refers to the pressure drop per unit cell averaged over the course of a single run, nondimensionalized with the surface tension scaling $\gamma'_{(o/a)}/R'$. In Fig. 8 the pressure drops required to drive the purified water benchmark runs in capillary tubing of two different inner diameters are presented against tube age, i.e., the number of days which have elapsed since a series of surfactant experiments was begun. The values of the nondimensional groups for the results reported in Fig. 8 are tabulated in Table II. The triangles in Fig. 8 represent pressure drop data for 0.155 cm i.d. runs and the squares 0.097 cm i.d. runs. The average over all the runs was 0.35. All the pressure drops reported in the figure fall within a $\pm$ 10% range of this value, and this reflects the nondimensional equivalence of the experiments done on the two different sized tubings: Note that for the clean surface flow regime the only nondimensional groups that are tube diameter dependent are the oil induction rate group (Ω), the aspect ratio (λ), and the Bond number (Bo) for the aqueous–oil interface. The former two groups are maintained equal in the experiments done on the two different sized tubings, and the latter, which measures the influence of gravitational forces to those of surface tension, is equal to 0.036 (for the 1 mm i.d. tubing). Bond numbers for the other two interfaces are equal to 0.29 and 0.034 for the oil–gas and aqueous–gas interfaces, respectively. As these values are small, gravitational effects are not that important and the difference between the Bond numbers between tubes should not significantly alter the nondimensional equivalence. Note that after it becomes impossible to sufficiently clean the tube to achieve the benchmark value for the pres-

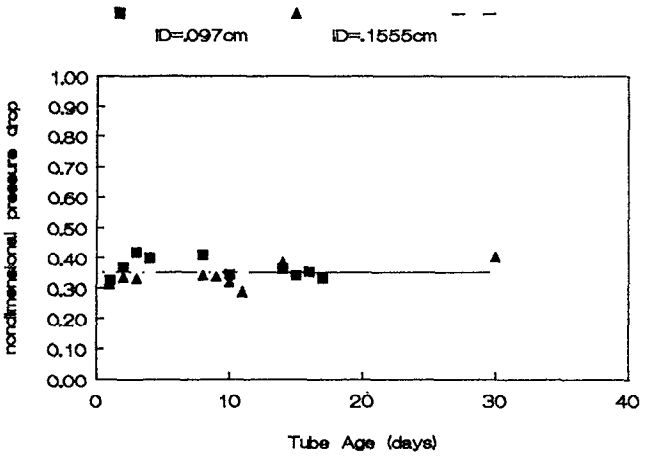

FIG. 8. Water benchmark runs: nondimensional pressure drop per unit cell required to drive the three-phase slug flow in the absence of added surfactant as a function of tubing age.

sure drop (i.e., after the tubing was exposed to highly elevated concentrations of surfactant or protein) the tubing is discarded.

As stated above, the average nondimensional pressure drop per cell over all runs in both series was 0.35; this number specifies the pressure drop over a pair of aqueous and air slugs in a unit cell nondimensionalized with the surface tension scaling $\gamma'_{(o/a)}/R'$. There are three principal contributions to this pressure drop: the capillary contributions due to the difference in curvature at the leading and trailing edges of the air and aqueous slugs and the pressure drop necessary to drive the recirculation of fluid within the aqueous segment itself. These pressure drops are marked in Fig. 1. A theoretical estimate for them may be constructed as follows.

Consider first the expression found by Bretherton to describe the pressure drop over a single long gas slug in a fluid-filled capillary tube at low capillary number:

$$\Delta P'_c/(\gamma'_{(o/n)}/R') = 4.52(3\,\mathrm{Ca}_{(o/n)})^{2/3}, \qquad (8)$$

where $\gamma'_{(o/n)} = \gamma'_{(o/a)}$ if the pressure drop over the aqueous slug is being estimated, and $\gamma'_{(o/n)} = \gamma'_{(o/g)}$ if that over the gas slug is being estimated. In Eq. (8) the capillary number $\mathrm{Ca}_{(o/n)}$ is defined using the interfacial tension $\gamma'_{(o/n)}$. Pressure drops in the flow of adjoining slugs, rather than isolated ones, have been studied by Ratulowski and Chang.[54] Their flow regime is one of adjoining gas slugs which move over a wetting fluid layer in a tube. Using an internal matching analysis in which the lubrication equations around the cylindrical sections are extended to the bubble ends and wetting inclusion regions, these authors find (to leading order) no correction to the isolated bubble expression. Hence the only drawback in using the Bretherton expression for the slug flow of this study is that it does not incorporate the influence of the slug viscosity on the aqueous slug capillary contributions. Park and Homsy,[55] in a reexamination of the fingering of an infinite (two-dimensional) viscous slug in a channel, established that, to leading order, the finger viscosity can be neglected in determining the capillary pressure drop and the axial drop in the film, as long as the ratio of the slug to continuous phase viscosity is less than $\mathrm{Ca}^{-1/3}$. Since the latter condition is clearly satisfied with respect to the aqueous slug in the connected flow of this study, the Bretherton expressions can be used with some confidence.

Using the capillary numbers detailed in Table II, $(P'_1 - P'_2 + P'_3 - P'_4)/(\gamma'_{(o/a)}/R')$ (the capillary contribution to the nondimensional pressure drop over the aqueous slug) is equal to 0.096, and $(P'_4 - P'_6)/(\gamma'_{(o/a)}/R')$ (the capillary contribution to the nondimensional drop over the gas slug) is equal to 0.062.

As demonstrated by Park and Homsy, the pressure drop caused by the recirculation of the liquid in the aqueous segment $(P'_2 - P'_3)$ is negligible to order $\mathrm{Ca}^{2/3}_{(o/a)}$ when κ^{-1} is smaller than $\mathrm{Ca}^{-1/3}_{(o/a)}$. A simple derivation which assumes uniaxial motion in the slug interior and film in the regions away from the slug ends shows that this contribution is of order Ca and can be approximated by

$$(P'_2 - P'_3)/(\gamma'_{(o/a)}/R') = \{8\lambda(1-\epsilon)/[\kappa\xi^2 + 2(1-\xi^2)]\}\mathrm{Ca}_{(o/a)}, \qquad (9)$$

where κ is the viscosity ratio of the oil to the aqueous solution, ξ is equal to $(1 - \bar{h}'/R')$, where $\bar{h}'$ is the average thickness of the annular oil film surrounding the aqueous segment. Since for small capillary numbers $\bar{h}'/R'$ is asymptotically close to zero, it is clear from (9) that to leading order, the pressure drop required to drive the aqueous core recirculation is simply $(P'_2 - P'_3)/(\gamma'_{(o/a)}/R') = [8\lambda(1-\epsilon)/\kappa]\mathrm{Ca}_{(o/a)}$ and is numerically equal to 0.065. The sum of the three contributions to the pressure drop is equal to 0.22, which is several percent lower than the measured value (0.35). This discrepancy is probably due to the presence of surface active impurities in the oil which retard the surface velocity and elevate the pressure drop. (Evidence for these impurities can be found in the dynamic interfacial tensions of a freshly created oil drop in water as measured by pendant drop tensiometry: With time, the interfacial tension slowly relaxes from 59 dyn/cm to approximately 55 dyn/cm indicating the slow diffusion toward the surface of a surface active impurity.) Also it should be noted that for a completely consistent estimate, the capillary pressure drops of order Ca, which can include the influence of the aqueous slug viscosity, should be included since the drop required to drive the recirculation begins at order Ca, and this term was included in the estimate. However, the order Ca corrections have not as yet been obtained in any theoretical studies.

B. Triton X-100 and Brij-35 results

In Fig. 9 data from the series of runs using Triton X-100 in the aqueous phase in tubes of 0.1555 and 0.097 cm i.d., respectively, are presented. The abscissa in the figure is the parameter $\Phi k/\phi(k)\mathrm{Pe}^{1/2}$ evaluated for the aqueous–oil interface. As C'_∞ is varied from $0\text{–}1.55\times10^{-8}$ g mole/cm^3 $[\Phi(1+k)\mathrm{Pe}^{1/2} < 0.035]$, the nondimensional pressure

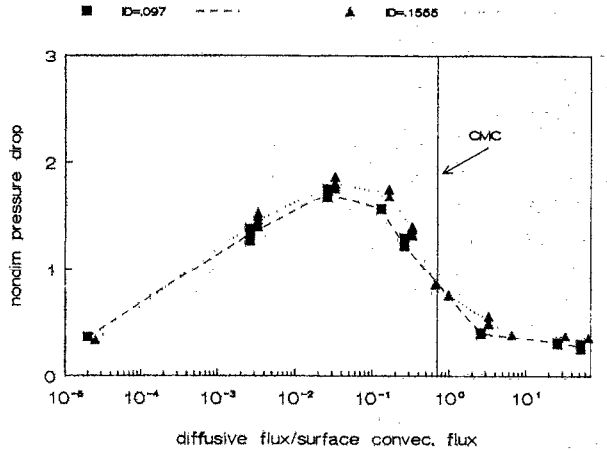

FIG. 9. Nondimensional pressure drop per unit cell as a function of the ratio of diffusive mass flux to the rate of surface convection for Triton X-100.

drop increases monotonically to a maximum value that is approximately five times greater than that required to drive the clean flow. In the concentration range the group $\Phi(1+k)\mathrm{Pe}^{1/2}$ increases monotonically, but is always less than 1.0. This small value reflects the fact that the bulk diffusion barriers are significant and thus at steady state surfactant has accumulated at the rear stagnation zone with little exchange with the bulk [i.e., $\nabla_s\cdot(\Gamma \mathbf{v}_s)\to 0$]. The Marangoni surface traction which arises due to the surfactant accumulation reduces the surface velocity since the traction is opposite to the flow. Since the surface velocity toward the rear stagnation zone is decreased in the long cylindrical section of the aqueous slug, the net hydrodynamic drag on the slug is increased. The slug or train velocity is maintained at a constant value during the experiments, so the pressure drop driving the flow must increase in order to overcome this increased drag opposing flow. This is why $\Delta P'$ increases from the clean value. Note also that as C'_∞ is increased, the bulk diffusion barriers begin to be reduced. In this concentration range, however, as C'_∞ increases the increased adsorption causes the surface velocity to be reduced along a larger region of the cylindrical surface, accounting for the increase of $\Delta P'$ with C'_∞.

The peak in the pressure drop occurs at 1.55×10^{-8} g mole/cm^3 Triton X-100 [$\Phi(1+k)\mathrm{Pe}^{1/2}=0.03$], and is equal to approximately 1.75. It is interesting to relate this maximum pressure to that required to drive a train with tangentially immobile interfaces in order to understand how fully retarded the interface is. By approximating the flow in the film by uniaxial motion, it can easily be shown that this axial pressure drop (denoted by $\Delta P'_f$) is given nondimensionally by $4(1-\epsilon)\lambda\ \mathrm{Ca}_{(o/a)}/(1-\xi^2)$, where $\xi=1-\bar{h}'/R'$. To estimate the film thickness around the aqueous slug, consider first the Bretherton asymptotic analysis for isolated bubbles with completely mobile surfaces: $\bar{h}'/R' = 1.337(\mathrm{Ca}_{(o/a)})^{2/3}$. The train flow results of Ratulowski and Chang indicate that the film thickness around the connected flow is given by Bretherton's expression multiplied by $1-(R'_c/R')$, where R'_c is the radial location of the inclusion cusp. Noting the results of Park and Homsy that as long as $\kappa^{-1}<\mathrm{Ca}_{(o/a)}^{-1/3}$, the influence of the slug viscosity on the leading order result is negligible, it can be concluded that an excellent approximation to the clean surface film thickness is $\bar{h}'/R' = 1.337[1-(R'_c/R')]\mathrm{Ca}^{2/3}$. Therefore the pressure drop along the wetting layer is given by

$$\frac{\Delta P'_f}{\gamma'_{(a/o)}/R'}=\frac{2(1-\epsilon)\lambda\ \mathrm{Ca}_{(o/a)}^{1/3}}{1.337[1-(R'_c/R')]}. \tag{10}$$

Using a value of R'_c/R' of 0.5 [cf. Figs. 7(a) and 7(b)], the result is a predicted pressure drop of the order of 10. It is therefore clear that even at the maximum, the aqueous–oil interface is far from being completely immobilized.

Instead of assuming a completely immobile interface, perhaps a more accurate way of estimating the maximum pressure drop is to equate the pressure drop that drives the aqueous slug, $(P'_1-P'_4)\pi R'^2$, to the maximum retarding Marangoni traction, $2\pi R'(\gamma'_{(o/a)}-\gamma'_{(o/a)\mathrm{CMC}})$. With this estimate, the maximum pressure drop across the aqueous slug ($\Delta P'_M$) is given by[56]

$$\Delta P'_M/(\gamma'_{(o/a)}/R') = 2\{\gamma'_{(o/a)}-\gamma'_{(o/a)\mathrm{CMC}}\}/\gamma'_{(o/a)}. \tag{11}$$

From the data given in Table I, this maximum nondimensional pressure drop required to move the aqueous slug is calculated to be 1.69. Adding to this the capillary pressure drop required to move the gas slug (previously calculated to be 0.062) results in a maximum pressure drop of 1.75, which is exactly equal to the maximally observed value (Fig. 9).

As the bulk concentration is increased in the range of 1.55×10^{-8}–3.1×10^{-5} g mole/cm^3 [$0.035\leqslant\Phi(1+k)\times\mathrm{Pe}^{1/2}\leqslant60$] the pressure drop required to drive the flow decreases fivefold due to the elimination of diffusion gradients in the bulk. The group $\Phi(1+k)\mathrm{Pe}^{1/2}$ varies from 0.035 to 60, indicating that within this bulk concentration range diffusion barriers in the sublayer to the interface have been completely eliminated.

Note that the CMC for Triton X-100 corresponds to a value of $\Phi(1+k)\mathrm{Pe}^{1/2}$ of 0.7 (cf. Fig. 9); half of the relaxation in pressure drop therefore takes place at concentrations above the CMC, and in the presence of micelles. The advent of micellization complicates the physicochemical picture, and some of the implications are discussed in the following section.

Since the clean surface pressure drop is recovered, the surface concentration is uniform and the interface is tangentially mobile. An interface that is completely tangentially mobile with uniform surface concentration in the absence of diffusion barriers can only be obtained if no desorption barriers exist. The ratio of desorption rate to that of surface convection, $\nu=\alpha' R'\lambda(1-\epsilon)/U'$, was found in Sec. III to be bounded from below by $O(10^{-2})$. If ν were on this order, however, the arguments presented in the Sec. III indicate that the clean surface pressure drop would not be recovered at elevated bulk concentration. Thus the reduction of the pressure drop to that required to drive the clean flow at ele-

vated C'_∞ therefore indicates that Triton X-100 has desorption kinetics faster than the $O(10^{-3}\ \text{sec}^{-1})$ lower bound inferred from the pendant drop experiments of Sec. III.

A surfactant-laden interface in the absence of bulk diffusion barriers in which surfactant adsorbs and desorbs freely behaves as if it were a clean interface in the tangential stress balance. The interface, however, is more easily deformed as the surface tension at these high concentrations is significantly less than that in the absence of surfactants. This will affect the capillary contribution to the pressure drop over the aqueous slug. Using the pressure drop expression obtained by Bretherton, the ratio of the pressure drop for the uniformly populated surface to that required to drive the clean flow should be the ratio of the interfacial tensions of the two surfaces to the one-third power. The interfacial tension at the aqueous–oil interface at and above the CMC is 9.2 dyn/cm. The ratio of the pressure drop required to drive the uniformly populated interface to that required to drive the clean flow as predicted by the Bretherton expression is 0.6. Therefore the capillary contribution to the pressure drop realized over the length of an aqueous segment at the highly elevated surfactant concentrations is 0.056. The contributions to the pressure drop owing to the capillary forces over the air segment and because of the internal circulation in the aqueous segment remain the same, as surfactants are not present at the air–oil interface and the viscosity of the aqueous solution remains constant throughout the concentration range considered. Therefore the pressure drop over a unit cell at the lower interfacial tension is estimated to be 0.183, or 0.84 times that required to drive the clean flow. In our experimental apparatus the pressure drop required to drive the concentrated surfactant solutions was less than that required to drive the clean flow in only one of the two series of experiments reported. The average nondimensional pressure drop at $\Phi(1+k)\text{Pe}^{1/2} = 60$, which corresponds to a C'_∞ of 3.1×10^{-5} g mole/cm^3, is 0.32, which is 0.91 times that required to drive the clean flow. Note that this agreement is only in the average sense: the pressure drop at this elevated k value decreased only for the 0.097 cm i.d. tubing. In the 0.097 cm i.d. tube the pressure drop required to drive the 3.1×10^{-5} g mole/cm^3 solution of Triton X-100 is 0.28, which is 0.8 times that required to drive the clean flow. The pressure drop required to drive the flow at this concentration in the 0.1555 cm i.d. Triton X-100 series was 0.36, which is approximately the same as the clean interface pressure drop.

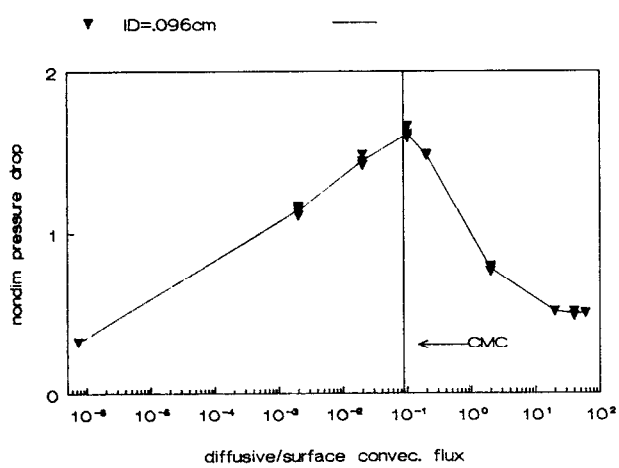

FIG. 10. Nondimensional pressure drop per unit cell as a function of the ratio of the diffusive mass flux to the rate of surface convection for Brij-35.

Figure 10 provides the results when the aqueous phase contains increasing concentrations of the Brig-35 surfactant; measurements were only obtained in the smaller diameter tubing. Again an improvement of surface mobility is evident, though, in contrast with the Triton X-100 results, the reduction in the pressure drop occurs after the CMC is reached, and this pressure drop does not fall below the clean surface value at very high C_∞. The maximum pressure drop is equal to 1.6, and this value again falls far below the tangentially mobile result of order 10 as given by Eq. (10). However, the estimate of the maximum pressure drop using the largest interfacial tension difference [Eq. (11)] gives (using the data of Table I) a value of 1.5, which is very close to the observed value as was the case with the Triton X-100 surfactant solutions.

C. Surfactant mass transfer and remobilization above the CMC

As has been mentioned previously, at converging stagnation points on the fluid particle surface the surface concentration is raised to values higher than the equilibrium value Γ'_0. Assuming for the purpose of these arguments that the sorption kinetics have already been established as fast, stagnation point concentration of adsorbed surfactant leads to adjoining sublayer concentrations of monomer that are higher than the bulk concentration of surfactant (away from the interface). Alternatively, regions on the surface sufficiently far away from the converging points have surface concentrations lower than the equilibrium value, and corresponding sublayer concentrations lower than the bulk value.

When the bulk concentration of surfactant reaches the CMC, monomer and micelle exist at equilibrium. (The CMC value is denoted here as C'_{CMC} and the corresponding equilibrium surface concentration by Γ'_{CMC}.) In the dynamic case, as the CMC is reached and passed, surface convection generates in the neighborhood of the converging stagnation point surface concentrations above Γ'_{CMC} and sublayer concentrations above C'_{CMC}. Because the sublayer concentration exceeds C'_{CMC}, micelles are present, and sublayer monomer in excess of C'_{CMC} can diffuse into the bulk or become incorporated into a micelle. The latter event locally elevates the micelle concentration above its equilibrium value, and micelles diffuse toward the bulk. To describe this second micelle incorporation-diffusion pathway for the removal of excess monomer, bulk convective diffusion equations should be formulated for the micelle as well as the mon

omer, with each of these expressions to include a kinetic term describing the incorporation of monomers into micelles.

Some attempts in this direction have been undertaken by Lucassen[8] in studying longitudinal waves, and Rillaerts and Joos[50] in examining surfactant adsorption onto an initially clean surface in a falling film experiment and an oscillating jet apparatus. The latter study is particularly relevant since micellar solutions of Triton X-100 were examined. Rillaerts and Joos find values for the first-order kinetic constant for exchange of monomer between the bulk and micelle to range from 4.5 $\sec^{-1}$ at twice the CMC to 608 $\sec^{-1}$ at ten times the CMC. As these values are sufficiently faster than the rate of convection on the fluid particle surface, $[\lambda R'(1-\epsilon)/U']^{-1}$, which is of the order of 0.1 $\sec^{-1}$, it is correct to assume that instantaneous equilibrium is achieved between monomer and micelle. The simplest characteristic to assume of this equilibrium is that the equilibrium monomer concentration is constant, and equal to the value at the CMC.

As adsorbed surfactant is swept to a surface stagnation point, the surface concentration is raised above the equilibrium value. For micellar solutions, this means above Γ'_{CMC}, the equilibrium surface coverage at the CMC. (Recall that above the CMC the equilibrium adsorption is constant and equal to the value at the CMC.) If it is assumed that the exchange between sublayer and surface is fast (a prerequisite for remobilization), the sublayer and surface are in equilibrium. The compaction of surfactant at the converging stagnation point raises the surface concentration above Γ'_{CMC}, and this causes the monomer concentration to rise above C'_{CMC}. However, because of the monomer–micelle equilibrium, monomer in excess of the CMC value is incorporated into micelles, and the sublayer concentration is maintained at the CMC value. Furthermore, as a result of sublayer–surface equilibrium, the surface is maintained at Γ'_{CMC}. Thus in the immediate neighborhood of the stagnation point no Marangoni stresses exist because the surface concentration is uniform.

Marangoni stresses arise away from the converging stagnation point. Away from this point, surface convection acts to reduce the surface concentration to values below Γ'_{CMC}. Through adsorption, the sublayer–surface equilibrium causes the sublayer concentration to be less than C'_{CMC}. Since the sublayer concentration is below the CMC, micelles disassociate and the region is devoid of micelles. The surface concentration is not uniform since micelles are not present underneath the surface to maintain a uniform subsurface concentration of monomer. Consequently, the surface concentration increases in the direction toward the stagnation point, and a retarding Marangoni stress is exerted.

In the micelle-free zone monomer diffuses toward the surface supplying the surfactant which later adsorbs and is convected toward the converging stagnation point. The micelle-free zone extends out away from the interface to a boundary where the bulk monomer concentration reaches C'_{∞} and micelles reappear. Here, in this outer region the monomer concentration is fixed, and micelles diffuse toward the boundary where they disassociate, and the monomer then proceeds through the micelle-free zone. The size of the micelle-free zone is determined by the length scale necessary for monomer diffusion in that zone to balance (at the boundary) micelle diffusion in the outer boundary. As the overall bulk concentration increases, the micelle concentration in the outer boundary increases, as does the diffusive flux. Consequently, the micelle-free zone shrinks and moves farther away from the stagnation point. Eventually this zone disappears, and the particle surface is of uniform surface concentration and therefore completely remobilized.

D. Protein results

In order to recover clean surface behavior at large $[\Phi k/\phi(k)]\mathrm{Pe}^{1/2}$, the ratio of desorption to convection, ν, has to be large as well. In the event that $\nu \leqslant O(1)$ clean surface behavior for large $[\Phi k/\phi(k)]\mathrm{Pe}^{1/2}$ is not possible. The experimental results of Sec. V B indicate that $\nu \gg 1$ for Triton X-100 and Brij-35 as clean interface behavior is recovered. In order to confirm that this observed relaxation of tangential stresses at the interface was due to the fast sorption kinetics of these polyethoxy surfactants, the protein BSA in solution was used to form the aqueous phase in the three-phase slug flow.

The desorption rate constant α' for BSA was estimated in Sec. III to be of the order $10^{-6}\ \sec^{-1}$, which is much slower that the convection rate $([\lambda R'(1-\epsilon)/U']^{-1})$ which is of order 0.1 $\sec^{-1}$ for the three-phase flow experimental conditions. Therefore, unlike Triton X-100 and Brij-35, because the rate of protein desorption is anticipated to be less than the convective rate, remobilization will not occur at the high bulk concentrations which demarcate the elimination of bulk diffusion barriers.

To illustrate this possibility, the protein bovine serum albumin was employed. The Frumkin kinetic constants for BSA (for primary adsorption onto air–water interface) are listed in Table I, and the parameter Φ necessary to compute the ratio of the diffusive to the convective rate is given in Table III. In Fig. 11 a graph of the nondimensional pressure drop per cell against $[\Phi k/\phi(k)]\mathrm{Pe}^{1/2}$ for a series of experiments in which BSA was used to form the aqueous phase in the three-phase slug flow is presented. The experiments were undertaken in 0.155 cm i.d. tube. Note that the intercept for zero weight percent protein (i.e., just the buffer solution) is ≈ 0.6, much higher than the intercept of 0.35 obtained in the clean water runs reported. This difference was attributed to the presence of impurities in the buffer. Note also that the pressure drop per cell for the protein increases throughout the value of $[\Phi k/\phi(k)]\mathrm{Pe}^{1/2}$ reported until at a value of 1 the pressure drop appears to become constant at a value of ≈ 2, and shows no subsequent decrease with increasing bulk concentration.. Data taken by Graham and Phillips indicates that at a bulk concentration of $1.5\times 10^{-10}\ \mathrm{g\ mole/cm^3}$, significant multilayer formation begins for BSA. (This bulk concentration corresponds to a value of $[\Phi k/\phi(k)]\mathrm{Pe}^{1/2} = 0.006$.) Multilayer formation and slow desorption most likely prevent the free interface behavior from being remobilized, as is explained below.

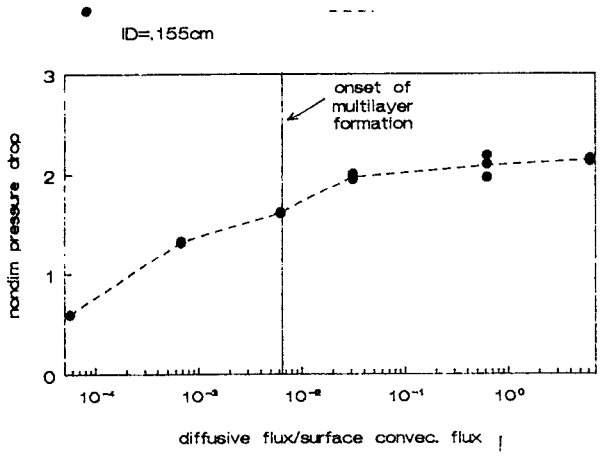

FIG. 11. Nondimensional pressure drop per unit cell as a function of the ratio of the diffusive mass flux to the rate of surface convection for the protein bovine serum albumin.

The initial increase in the pressure drop required to drive the flow with increasing C'_∞ can be explained as before. Protein adsorbs onto the interface and is convected along the length of the cylindrical region by interfacial convection. Since desorption is slow in comparison to convection, protein accumulates in this region, giving rise to Marangoni tractions which resist the flow, increasing the drag. As C'_∞ of protein is increased, the increased adsorption allows the surface velocity to be retarded along more of the cylindrical region of the aqueous slug, accounting for the increased pressure drop throughout the region of $[\Phi k/\phi(k)]\mathrm{Pe}^{1/2} < 1$ reported in Fig. 11.

For BSA in the range of $[\Phi k/\phi(k)]\mathrm{Pe}^{1/2} > 1$, diffusion barriers in the sublayer to the surface should have dissipated appreciably by the pressure drop required to drive the flow remains elevated. In this concentration range, the surfactant distribution is determined solely by the desorption kinetics. It is important to note that the plateau value (approximately 2) is less that the value of 10 estimated earlier for a completely immobilized aqueous–oil interface. The fact that the plateau value is less than the completely immobilized value indicates that the desorption rate, while slow compared to convection, is not zero. If the desorption rate were indeed zero, then protein would collect in a stagnant cap that would grow outward as the bulk concentration is increased until a completely immobilized interface is realized. In the case of the polyethoxy surfactants, an accurate measure of the maximum was obtained by equating the pressure drop to the largest realizable surface pressure [cf. Eq. (11)]. Experiments by Graham and Phillips[44] at the *n*-decane–water interface indicate that the largest surface pressure the protein BSA can exert at that interface is 18 dyn/cm (similar to that at the air–water interface as reported in Table I). Using this value in (11) and correcting for the gas slug capillary contribution results in a value of only 0.66, significantly less than the observed value of 2. It is possible that because of the size of the protein molecule, surface viscosity effects, not consequential for the smaller-size polyethoxy surfactants, are important and may account for the elevated value observed.

VI. CONCLUSIONS AND IMPLICATIONS

In this study experimental evidence was presented which indicates that the interfaces of moving fluid particles can remain unhindered in the presence of a single adsorbed surfactant if, relative to the rate of surface convection, the surfactant has fast desorption kinetics, and is present in bulk concentrations high enough so that diffusive boundary layers are depressed, and the rate of bulk diffusion becomes fast. The flow regime used to establish this result is a capillary train flow of alternating aqueous and gas slugs moving over a fluorocarbon wetting layer. In this flow, the retarding effects of adsorbed surfactant on surface velocity are strongly reflected in changes in the driving pressure required to maintain constant slug velocity. Surface adsorbers were dissolved in the aqueous phase of the three-phase slug flow; convection of surfactant to the slug rear created a region of reduced surface mobility that extended, with increasing bulk concentration, into the long cylindrical part of the aqueous–oil interface. Loss of mobility of this part of the interface created large retarding shearing stresses in the thin wetting layer around the slug, and these stresses increased the pressure drop required to move the train at a constant velocity.

The remobilizing surfactants used in this study were the polyethoxy surfactants Triton X-100 and Brij-35; pendant drop tensiometry experiments showed these surfactants to be good candidates for remobilization because their desorption rates are potentially high. At highly elevated concentrations of Triton X-100 or Brij-35, the three-phase slug flow behaved hydrodynamically as it would in the absence of added surfactant, save that it had a uniform, reduced surface tension. As a counter example, the presumed slowly desorbing protein BSA was dissolved in the aqueous phase. Even at concentrations where bulk diffusion barriers of BSA had been eliminated, the pressure drop required to drive the three-phase slug flow remained at its elevated value, indicating that both fast desorption kinetics as well as the elimination of diffusion barriers in the bulk are necessary for a surfactant to remobilize a retarded surface flow.

The major implication of this study concerns the remobilization of fluid–fluid interfaces in fluid particle flows retarded by adsorption of surfactant impurities in the system. As mentioned in the Introduction, this idea is described and studied in detail in a companion paper[6] and therefore only a few remarks will be given here. The commonly observed effect of surfactant impurities in multiphase fluid systems is an increase in the drag opposing the flow, resulting in a decreased particle velocity. A well-known example is the retardation of the terminal velocity attained by moving fluid droplets in an infinite medium where a surfactant is present in trace amounts in either the droplet or bulk phase (cf. Levich[15]). Within the context of this study, the following reasons can be posited for the observed reduction in terminal velocity. If the surface active impurity is present in low

enough concentration so that the group $[\Phi k/\phi(k)]\mathrm{Pe}^{1/2}$ is small, i.e., there are diffusion barriers in the bulk, surface concentration gradients will develop. If the surface active impurity has slow desorption kinetics, surface concentration gradients will again develop. In either of the above cases, the results of this study indicate the possibility that if a surfactant with fast desorption kinetics is added in high enough concentration so that its adsorption and diffusion rates are fast, such a surfactant can preferentially adsorb on the fluid interfaces, displacing the retarding impurity or not allowing it to adsorb. The surface, now populated with a surfactant which freely exchanges with the subsurface, is mobile and the droplet settles at the unretarded terminal velocity. Experiments using the three-phase flow to validate the idea of competitive adsorption as a means of remobilization are provided in the companion study.

ACKNOWLEDGMENT

This work was supported in part by Grant No. DE-FGO2-88ER13820 from the Engineering Research Program of the Office of Basic Energy Sciences, U.S. Department of Energy.

[1]See, for example, F. H. Garner and A. H. P. Skelland, Chem. Eng. Sci. **4**, 149 (1955); E. R. Elzinga and J.T. Banchero, AIChE J. **7**, 394 (1961); W. S. Huang and R. C. Kintner, AIChE J. **15**, 735 (1969); A. Beitel and W. J. Heideger, Chem. Eng. Sci. **26**, 711 (1971).
[2]For example, B. P. Radoev, D. S. Dimitrov, and I. B. Ivanov, Colloid Polym. Sci. **252**, 50 (1974); I. B. Ivanov and D. S. Dimitrov, in *Thin Liquid Films*, edited by I. B. Ivanov (Marcel Dekker, New York, 1988).
[3]H. S. Kim and R. S. Subramaniam, J. Colloid Interface Sci. **127**, 417 (1989); H. S. Kim and R. S. Subramaniam, J. Colloid Interface Sci. **130**, 112 (1989).
[4]G. Hirasaki and J. B. Lawson, SPE J. **25**, 176 (1986).
[5]G. M. Ginley and C. J. Radke, ACS Symp. Ser. **396**, 480 (1989).
[6]K. Stebe and C. Maldarelli, submitted to J. Colloid Interface Sci.
[7]J. Lucassen, Trans. Faraday Soc. **64**, 2221, 2230 (1968); J. Lucassen and M. van den Tempel, *ibid.* **27**, 1283 (1972); J. Lucassen and G. T. Barnes, J. Chem. Soc. Faraday 1 **68**, 2129 (1972); J. Lucassen and D. Giles, *ibid.*, **71**, 217 (1975).
[8]J. Lucassen, Faraday Discuss. Chem. Soc. **59**, 76 (1976).
[9]S. Y. Lin, K. McKeigue, and C. Maldarelli, AIChE J. (in press).
[10]P. Savic, Report No. MT-22, Division of Mechanical Engineering, National Research Council of Canada, 1953.
[11]R. E. Davis and A. Acrivos, Chem. Eng. Sci. **21**, 681 (1966).
[12]J. F. Harper, J. Fluid Mech. **58**, 539 (1973).
[13]S. S. Sadahl and R. E. Johnson, J. Fluid Mech. **126**, 237 (1982).
[14]A. Frumkin and V. G. Levich, Zh. Fiz. Khim. **21**, 1183 (1947).
[15]V. G. Levich, *Physicochemical Hydrodynamics* (Prentice–Hall, Englewood Cliffs, NJ, 1962), pp. 409–420.
[16]J. Newman, Chem. Eng. Sci. **22**, 83 (1966).
[17]M. L. Wasserman and J. C. Slattery, AIChE J. **15**, 533 (1969).
[18]D. A. Saville, Chem. Eng. J. **5**, 251 (1973).
[19]J. F. Harper, J. Mech. Appl. Math. **27**, 87 (1974).
[20]J. F. Harper, Adv. Appl. Sci. **35**, 343 (1982).
[21]M. D. Le Van and J. Newman, AIChE J. **22**, 695 (1976).
[22]M. D. Le Van and J. A. Holbrook, Chem. Eng. Commun. **20**, 191 (1982).
[23]M. D. Le Van and J. A. Holbrook, Chem. Eng. Commun. **20**, 273 (1982).
[24]M. D. Le Van and J. Holbrook, J. Colloid Interface Sci. **131**, 242 (1989).
[25]S. K. Agrawal and D. T. Wasan, Chem. Eng. J. **18**, 215 (1979).
[26]M. D. Le Van, J. Colloid Interface Sci. **83**, 11 (1981).
[27]Y. J. Horton, T. R. Fritsch, and R. C. Kintner, Can. J. Chem. Eng. 143 (1965).
[28]R. M. Griffith, Chem. Eng. Sci. **17**, 1057 (1962).
[29]F. P. Bretherton, J. Fluid Mech. **10**, 166 (1961).
[30]E. I. Shen and K. S. Udell, J. Appl. Mech. **52**, 253 (1985).
[31]D. A. Reinelt and P. G. Saffman, SIAM J. Sci. Stat. Comput. **6**, 542 (1985).
[32]H. Westborg and O. Hassager, J. Colloid Interface Sci. **133**, 135 (1989).
[33]M. J. Martinez and K. S. Udell, Trans. ASME E: J. Appl. Mech. **56**, 211 (1989).
[34]M. J. Martinez and K. S. Udell, J. Fluid Mech. **210**, 565 (1990).
[35]F. Fairbrother and A. E. Stubbs, J. Chem. Soc. **1**, 527 (1935).
[36]R. N. Marchessault and S. J. Mason, Ind. Eng. Chem. **52**, 79 (1960).
[37]H. L. Goldsmith and S. G. Mason, Colloid Sci. **18**, 237 (1963).
[38]J. D. Chen, J. Colloid Interface Sci. **109**, 341 (1986).
[39]L. W. Schwartz, H. M. Princen, and A. D. Kiss, J. Fluid Mech. **172**, 259 (1986).
[40]E. Herbolzheimer, AIChE Annual Meeting, New York, November 1987, Paper No. 68j.
[41]J. Ratulowski and H.-C. Chang, J. Fluid Mech. **210**, 303 (1990).
[42]M. Delaunay, These de Doctorat, Universite de Technologie de Compiegne, 1985.
[43]D. Barthes-Biesel, N. Moulai-Mostefa, and E. Meister, in *Proceedings of the Physicochemical Hydrodynamics NATO Conference* (La Rabida, Spain, 1986).
[44]D. E. Graham and M. C. Phillips, J. Colloid Interface Sci. **70**, 403, 415 (1978).
[45]R. Guzman, R. G. Carbonell, and P. K. Kilpatrick, J. Colloid Interface Sci. **114**, 536 (1986).
[46]F. MacRitchie and A. E. Alexander, J. Colloid Sci. **18**, 453 (1962).
[47]F. MacRitchie and A. E. Alexander, J. Colloid Sci. **18**, 458 (1962).
[48]L. Ter Minassian-Saraga, J. Colloid Interface Sci. **80**, 393 (1981).
[49]See, for example, C. Huh and R. L. Reed, J. Colloid Interface Sci. **91**, 472 (1984); Y. Rotenberg, L. Boruvka, and A. W. Neuman, *Ibid.* **93**, 169 (1983); H. H. Girault, D. J. Schiffren, and B. D. V. Smith, *Ibid.* **101**, 257 (1984); H. H. Girault, D. J. Schiffren, and B. D. V. Smith, J. Electroanal. Chem. **137**, 207 (1984); C. I. Chiwetelu, V. Hornof, and G. H. Neale, J. Colloid Interface Sci. **125**, 586 (1988).
[50]E. Rillaerts and P. Joos, J. Phys. Chem. **86**, 3471 (1982).
[51]J. Van Havenbergh and P. Joos, J. Colloid Interface Sci. **95**, 172 (1983).
[52]J. Van Hunsel, G. Bleys, and P. Joos, J. Colloid Interface Sci. **114**, 432 (1986).
[53]J. Van Hunsel, D. Vollhardt, and P. Joos, Langmuir **5**, 528 (1989).
[54]J. Ratulowski and H. C. Chang, Phys. Fluids A **1**, 1642 (1989).
[55]C. W. Park and G. M. Homsy, J. Fluid Mech. **139**, 291 (1983).
[56]R. Probstein, *Physicochemical Hydrodynamics: An Introduction* (Butterworths, London, 1989), pp. 308–311.
[57]"The Physical Properties of Fluorinert Brand Electronic Liquids," 3M Co., Minneapolis, Minnesota.